Short title: The function of terminal oxidases in cyanobacteria

Corresponding author details

Yagut Allahverdiyeva

Laboratory of Molecular Plant Biology, Department of Biochemistry, University of Turku, Turku, FI-20014, Finland

allahve@utu.fi

Research area: Primary: Membranes, transport and biogenetics

Secondary: Biochemistry and metabolism

Distinguishing the roles of thylakoid respiratory terminal oxidases in the cyanobacterium *Synechocystis* sp. PCC 6803[1]

Maria Ermakova[*], Tuomas Huokko[*], Pierre Richaud, Luca Bersanini, Christopher J. Howe, David J. Lea-Smith, Gilles Peltier, Yagut Allahverdiyeva[#]

Laboratory of Molecular Plant Biology, Department of Biochemistry, University of Turku, Turku, FI-20014, Finland (M.E., T.H., L.B., Y.A.);
Commissariat à l'Energie Atomique et aux Energies Alternatives, Institut de Biologie Environnementale et de Biotechnologie, Laboratoire de Bioénergétique et Biotechnologie des Bactéries et Microalgues, Cadarache, Saint-Paul-lez-Durance, F-13108, France (P.R., G.P.);
Centre National de la Recherche Scientifique, Biologie Végétale et Microbiologie Environnementales, Unité Mixte de Recherche 7265, F-13108 Saint-Paul-lez-Durance, France (P.R., G.P.);
Aix Marseille Université, Biologie Végétale et Microbiologie Environnementales, Unité Mixte de Recherche 7265, Marseille, F-13284, France (P.R., G.P.);
Department of Biochemistry, University of Cambridge, UK (D.J.L-S., C.J.H).

* these authors contributed equally to this work

One-sentence summary: Electron sinks, comprising the O_2 utilizing respiratory terminal oxidases and flavodiiron proteins, contribute to photoprotection and regulation of photosynthesis under light in cyanobacteria.

List of author contribution: Y.A. designed the research, M.E., T.H., P.R., L.B. performed the experiments, analyzed the data; C.J.H. and P.G.P. contributed to the analytical tools; D.J.L-S contributed to the data analysis and analytical tools; M.E., T.H., D.J.L-S. and Y.A. wrote the article.

Funding: [1]This work was financially supported by the Academy of Finland Finnish Centre of Excellence in Molecular Biology of Primary Producers (2014-2019) project # 271832 and by the Kone Foundation (to Y.A.). L.B. was supported by the Alfred Kordelin

Foundation, D.J.L-S by the Environmental Services Association Education Trust. Support was also provided by the HélioBiotec platform, funded by the European Union (European Regional Development Fund), the Région Provence Alpes Côte d'Azur, the French Ministry of Research, and the CEA.

[#] corresponding author: Yagut Allahverdiyeva, e-mail: allahve@utu.fi

Abstract

Various O_2-utilizing electron sinks, including the soluble flavodiiron proteins (Flv1/3), and the membrane-localized respiratory terminal oxidases (RTOs), cytochrome *c* oxidase (Cox) and quinol oxidase (Cyd), are present in the photosynthetic electron transfer chain of *Synechocystis* sp. PCC 6803. However, the role of individual RTOs and their relative importance compared to other electron sinks is poorly understood, particularly under light. Via membrane inlet mass spectrometry gas-exchange, chlorophyll *a* fluorescence, P700 analysis and inhibitor treatment of wild-type and various mutants deficient in RTOs, Flv1/3 and photosystem I, we investigated the contribution of these complexes to the alleviation of excess electrons in the photosynthetic chain. For the first time we demonstrated the activity of Cyd in O_2 uptake under light, although it was detected only upon inhibition of electron transfer at the cytochrome b_6f site and in Δ*flv1/3* under fluctuating light conditions, where linear electron transfer was drastically inhibited due to impaired PS I activity. Cox is mostly responsible for dark respiration and competes with P700 for electrons under high light. Only the Δ*cox*/*cyd* double mutant, but not single mutants, demonstrated a highly reduced PQ pool in darkness and impaired gross O_2 evolution under light, indicating that thylakoid-based RTOs are able to compensate partially for each other. Thus both electron sinks contribute to alleviation of excess electrons under illumination: RTOs continue to function under light, operating on slower time ranges and on a limited scale, whereas Flv1/3 responds rapidly as a light-induced component and has greater capacity.

Cyanobacteria (oxygenic photosynthetic bacteria) inhabit a range of highly variable aquatic and terrestrial environments, which are diverse in light and in the availability of nutrients. With the exception of *Gloeobacter* species, all cyanobacteria contain a series of internal thylakoid membranes, where a photosynthetic electron transport chain (ETC) is localized. This ETC consists of four major protein complexes: photosystem II (PS II), cytochrome b_6f (Cyt b_6f), photosystem I (PS I) and ATP synthase, similar to that of eukaryotic photosynthetic organisms (Fig. 1). The photosynthetic electron transfer chain provides energy (ATP) and reducing equivalents (reduced ferredoxin (Fd), NADPH) for carbon anabolism and other vital processes.

Following absorption of photons by the large external light-harvesting antenna, the phycobilisome, the excitation energy is directed to the reaction centers of PS II and PS I, where charge separation occurs. In PS II, this process is followed by splitting of water to molecular oxygen and protons, which are released into the lumen, and extraction of electrons for the reduction of $P680^+$. Electrons ejected from P680, the primary donor of PS II, are forwarded to pheophytin, then to plastoquinone molecules (PQ), Q_A and Q_B. Following double reduction and protonation, plastoquinol (PQH_2) diffuses from the Q_B pocket into the membrane. PQH_2 is oxidized by Cyt b_6f, resulting in proton translocation to the lumen and electron transfer to the lumen-localized soluble electron carriers, plastocyanin (Pc) or cytochrome c_6 (Cyt c_6). These small proteins donate electrons to $P700^+$, the oxidized primary electron donor of PS I. Electrons extracted from P700 during charge separation are transferred via a chain of cofactors incorporated in PS I to Fd, a soluble electron carrier on the cytosolic side of the thylakoid membrane. The Fd:$NADP^+$ oxidoreductase (FNR) concludes the linear electron transport chain by catalyzing the formation of NADPH. A proton gradient established during photosynthetic electron transfer is used by ATP synthase for the production of ATP.

In the model cyanobacterium *Synechocystis* sp. PCC 6803 (hereafter *Synechocystis*) the thylakoid membrane is not just the site of photosynthesis but also respiration (reviewed in Vermaas, 2001; Mullineaux, 2014a; Lea-Smith et al., 2016). The respiratory electron transfer chain transfers electrons extracted from organic molecules into the PQ pool. NAD(P)H dehydrogenase-like complex type 1 (NDH-1), succinate dehydrogenase (SDH) and possibly one to three different NAD(P)H dehydrogenases type 2 (NDH-2) may participate in PQ pool reduction (Mi et al., 1992; Ohkawa et al., 2000; Cooley et al., 2000;

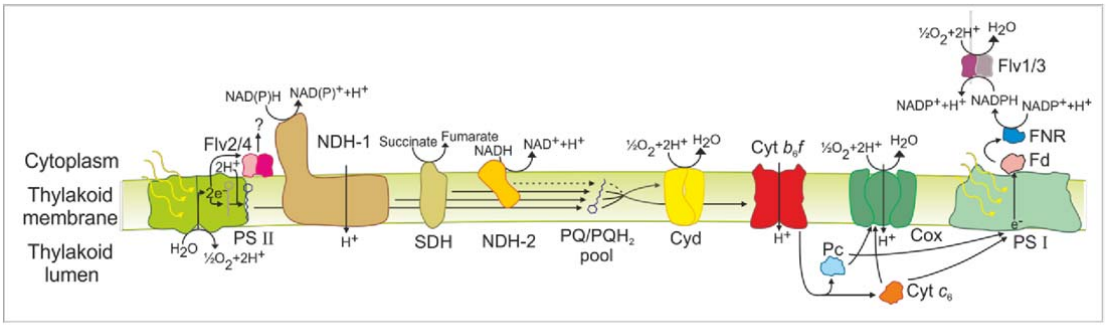

Figure 1. Schematic diagram of the thylakoid membrane-localized photosynthetic and respiratory electron transfer chains. Lines indicate electron transport; dotted lines indicate possible but poorly characterized electron transfer pathways. PS II, Photosystem II; Flv2/4, Flavodiiron proteins 2/4; Flv1/3, Flavodiiron proteins 1/3; PQ, plastoquinone; PQH_2, plastoquinol; Cyt b_6f, cytochrome b_6f complex; Pc, plastocyanin; Cyt c_6, cytochrome c_6; PS I, Photosystem I; Fd, ferredoxin; FNR, ferredoxin-$NADP^+$ oxidoreductase; NDH-1, NAD(P)H dehydrogenase-like complex type 1; SDH, succinate dehydrogenase; NDH-2, NAD(P)H dehydrogenase type 2; Cyd, cytochrome *bd* quinol oxidase; Cox, cytochrome *c* oxidase.

Howitt et al., 1999). PQH_2 oxidation can then occur via either Cyt b_6f or respiratory terminal oxidases (RTOs). In *Synechocystis*, the cytochrome *bd* quinol oxidase (Cyd), encoded by *cydAB*, reduces O_2 with electrons presumably taken directly from the PQ pool (Berry et al., 2002). Although Cyd does not pump protons across the membrane, it contributes to the thylakoid membrane potential by releasing protons from PQH_2 oxidation into the lumen, and by generating water using protons removed from the cytoplasm (reviewed in Hart et al., 2005). The aa_3-type cytochrome *c* oxidase complex (Cox), encoded by *coxBAC*, is situated only in the thylakoid membrane and can accept electrons from Pc and Cyt c_6 (Howitt and Vermaas, 1998; Nomura et al., 2006; Lea-Smith et al., 2013). Therefore, Cyt b_6f, the PQ pool and Pc/Cyt c_6 are shared by both the photosynthetic and respiratory electron transfer chains (Scherer, 1990). Cox is present in all cyanobacteria sequenced thus far (Pils and Shmetterer, 2001; Lea-Smith et al., 2013). Based on similarity with better characterized aa_3-type cytochrome *c* oxidase complexes from other bacteria, Cox can potentially couple the transfer of electrons to O_2 with the translocation of protons across the membrane (Iwata et al., 1995; Brändén et al., 2006).

An additional electron transport chain is localized in the cytoplasmic membrane, which lacks Cox (Huang et al., 2002) and Cyt b_6f (Schultze et al., 2009). This simpler pathway consists of electrons donated to PQ by NDH-2 and/or SDH, followed by transfer from

149 PQH_2 to RTOs. Localization of Cyd in the thylakoid membrane has been confirmed but
150 this complex may also be present in the cytoplasmic membrane (Howitt and Vermaas,
151 1998; Berry et al., 2002). Another RTO, the alternative oxidase complex (ARTO), encoded
152 by *ctaCIIDIIEII,* probably oxidizes the PQ pool and has been localized only to the
153 cytoplasmic membrane in *Synechocystis* (Huang et al., 2002; Pisareva et al., 2007). Thus
154 ARTO does not have a significant impact on photosynthetic electron transfer (Abramson et
155 al., 2000; Lea-Smith et al., 2013). However, a recent study suggested a possible role for
156 ARTO in reductive Fe uptake (Kranzler et al., 2014). An additional quinol oxidase, which
157 is closely related to the plastid terminal oxidase (PTOX) of plants, has been identified in a
158 range of cyanobacteria but is not present in *Synechocystis* (McDonald et al., 2011).
159
160 The main role of RTOs is to provide metabolic energy required during dark periods
161 (Matthijs and Lubberding, 1988). RTOs are not essential in *Synechocystis* when cells are
162 subjected to continuous moderate or high light (Lea-Smith et al., 2013, Howitt and
163 Vermaas, 1998; Pils and Schmetterer, 2001), or 12 h dark/12 h moderate light (40 μmol
164 photons m^{-2} s^{-1}) cycle regimes (Lea-Smith et al., 2013). However, the presence of Cox is
165 essential for viability under low light (Kufryk and Vermaas, 2006) and the presence of at
166 least one thylakoid-based RTO (Cyd or Cox) is required for survival under a 12 h dark/12
167 h high light (150 μmol photons m^{-2} s^{-1}) square cycle regime (Lea-Smith et al., 2013).
168
169 Studies of RTO mutants by gas-exchange under light are complicated in oxygenic
170 photosynthetic organisms, due to the O_2 evolving activity of PS II and the existence of
171 other processes capable of O_2 photoreduction. Flavodiiron proteins Flv1 and Flv3 are
172 responsible for the majority of O_2 uptake in the light in cyanobacteria (Allahverdiyeva et
173 al., 2011; Helman et al., 2003, 2005). These proteins likely form a functional couple
174 (Flv1/3) and reduce O_2 directly to water, conceivably, using NADPH formed as a result of
175 linear electron transfer (Vicente et al., 2002; Helman et al., 2003). Moreover,
176 cyanobacteria possess an active photorespiratory metabolism (Eisenhut et al., 2006, 2008)
177 and photorespiratory O_2 uptake plausibly contributes to the total O_2 uptake in the light and
178 in particular during C_i limitation (Allahverdiyeva et al., 2011). Therefore, the role of
179 individual RTOs and their relative importance compared to other electron sinks under light
180 conditions is poorly studied. In this work we used wild-type (WT) and various mutants of
181 *Synechocystis* in combination with specific inhibitors targeting electron transfer chain
182 components, to address the role of RTOs in the light. We demonstrate that Cyd is the key

183 RTO under light, capable of light-induced O_2 uptake under sub-optimal conditions. By
184 contrast, Cox is responsible for the majority of dark respiration but can also contribute to
185 regulation of electron flow to PS I under light in specific cases.
186
187

RESULTS

Light-induced O_2 uptake in *Synechocystis* cells in the absence and presence of inhibitors.

For a precise study of O_2 uptake in *Synechocystis* cells we used Membrane Inlet Mass Spectrometry (MIMS) and $^{18}O_2$-enriched O_2. In contrast to a classical oxygen electrode, which only measures net O_2 production under illumination, MIMS analysis can differentiate between gross O_2 produced by PS II and O_2 uptake under illumination based on increase of $^{16}O_2$ and decrease of $^{18}O_2$, respectively, in the reaction medium. When O_2 exchange was monitored in cultures during dark to light (400 μmol photons m^{-2} s^{-1}) transition, the WT demonstrated strong O_2 uptake of 34.6±6.7 μmol O_2 [mg Chl]$^{-1}$ h^{-1} under illumination, which was drastically higher than the O_2 uptake of the cells in darkness (8.3±1.2 μmol O_2 [mg Chl]$^{-1}$ h^{-1} (Fig. 2, Fig. S1, the averaged values and SDs are provided in Table 1). The difference between light and dark O_2 uptake rates is defined as the light-induced O_2 uptake rate. The Δ*flv1/3* mutant lacking the Flv1 and Flv3 proteins demonstrated a slightly higher O_2 uptake rate in darkness than the WT (10.8±1.6 μmol O_2 [mg Chl]$^{-1}$ h^{-1}), and a similar O_2 uptake rate in the light to that in darkness (Fig. S1). Thus, a strong light-induced O_2 uptake component observed in the WT was missing in the Δ*flv1/3*. This was in line with previous reports, demonstrating that O_2 uptake in WT *Synechocystis* was strongly stimulated in the light due to Flv1/3 activity occurring downstream of PS I (Helman et al., 2003, 2005; Allahverdiyeva et al., 2011, 2013, Mustila et al. 2016).

To investigate a possible role of RTOs functioning at the PQ pool level and to exclude contribution of the Flv1/3 to light-induced O_2 uptake, we performed MIMS experiments in the presence of 2,5-dibromo-6-isopropyl-3-methyl-1,4-benzoquinone (DBMIB), an inhibitor of PQH_2 oxidation at the site of Cyt b_6f (Trebst et al., 1970; Yan et al., 2006). In WT cells in the presence of DBMIB, the dark O_2 uptake rate was 10.1±1.5 μmol O_2 [mg Chl]$^{-1}$ h^{-1}, whereas in the light the rate of total O_2 uptake was two-fold higher than that in darkness (21.1±2.8 μmol O_2 [mg Chl]$^{-1}$ h^{-1}) (Fig. 2, Table 1). This demonstrates that a strong light-induced O_2 uptake is occurring in WT cells in the presence of DBMIB. To clarify the origin of this O_2 uptake we supplemented the cells, in addition to DBMIB, with 2,6 dichloro-*p*-benzoquinone (DCBQ), an artificial acceptor of electrons from PS II (Graan and Ort, 1986). Under these conditions, light-induced O_2 uptake was completely

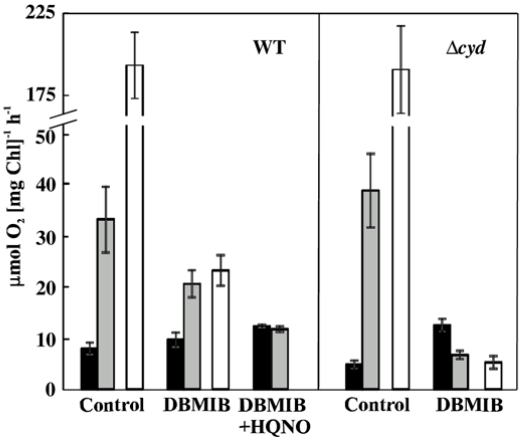

Figure 2. The rates of O_2 exchange in the WT and Δ*cyd* mutant cells incubated in darkness for 5 min and then illuminated with a strong white light (400 μmol photons m^{-2} s^{-1}) for the next 5 min. Black bars and grey bars indicate the rates of total O_2 uptake by cells in darkness and under the light, respectively; white bars indicate the gross O_2 production rate. Measurements were performed either in the absence of inhibitors (control) or in the presence of DBMIB or DBMIB + HQNO. Mean ± SD, n=3-5.

eliminated (Fig. S2A), implying strong competition between DCBQ and an unknown acceptor which can mediate the light-driven flow of electrons to O_2.

Importantly, in the presence of DBMIB, the gross O_2 evolution rate of WT cells decreased significantly (from 193.3±20.1 μmol O_2 [mg Chl]$^{-1}$ h^{-1} in the control cells to 24.2±3.1 μmol O_2 [mg Chl]$^{-1}$ h^{-1}, Fig. 2, Table 1), becoming nearly equal to the total O_2 uptake rate under the light. Consequently, the rate of net photosynthesis in the presence of DBMIB was close to zero (Table 1).

Next we used 2-n-heptyl-4-hydroxyquinoline N-oxide (HQNO), an inhibitor of Cyd (Pils et al., 1997). Supplementation of the DBMIB-treated cells with HQNO also completely eliminated the light-induced component of O_2 uptake (Fig. 2, Table 1). Thus the rate of O_2 uptake was observed to be similar between darkness and light, suggesting that Cyd is responsible for the light-induced fraction of O_2 uptake under the studied conditions. Addition of HQNO alone to the WT cells did not significantly affect total O_2 uptake under light (Fig. S2B), presumably due to the compensatory effect of other O_2 consuming pathways, such as Cox and Flv1/3.

It is important to note that the addition of DBMIB also increased dark O_2 uptake in WT *Synechocystis* cells (from 8.3±1.2 μmol O_2 [mg Chl]$^{-1}$ h^{-1} to 10.1±1.5 μmol O_2 [mg Chl]$^{-1}$ h^{-1}, Table 1), which is in line with a previous report (Zhang et al., 2013). This result raises a question whether DBMIB itself could act as an electron shuttle to O_2 (Bukhov et al.,

2003; Belatik et al., 2013), thus making interpretations difficult. In order to clarify the origin of increased O_2 uptake in the presence of DBMIB, the WT cells were further treated with KCN, which is an inhibitor of both Cyd and Cox (Howitt and Vermaas 1998). Addition of KCN to the DBMIB-treated WT cells completely abolished the light-induced component of O_2 uptake, suggesting a role for RTOs (Fig. S2C). However O_2 uptake in darkness decreased only slightly in the presence of KCN, demonstrating a residual O_2 uptake with a rate of about 7.4 μmol O_2 [mg Chl]$^{-1}$ h^{-1} occurring similarly under both darkness and light conditions in DBMIB supplemented cells (Fig. S2C). This suggests the existence of "background" O_2 uptake in the presence of DBMIB. Importantly this "background" O_2 uptake is insensitive to light, therefore would not affect the interpretation of light induced O_2 uptake in the WT. To clarify further the effect of this compound, we measured O_2 evolution rates of WT cells supplemented with different DBMIB concentrations using a Clark-type electrode. With increasing DBMIB concentrations the net O_2 production decreased gradually to almost zero at a concentration of 25 μM DBMIB (Fig. S2D), which is in line with the MIMS experiments (Table 1), and suggests that DBMIB act as an electron transfer inhibitor in *Synechocystis* cells. Our results differ from Belatik et al. (2013), which describe high O_2 production rates even at low DBMIB concentrations, and concluded that DBMIB could act as electron acceptor for PS II in spinach thylakoids. This discrepancy could be due to different experimental set ups and the different organisms used.

Light-induced O_2 uptake in *Synechocystis* cells deficient in RTOs.

In order to confirm the results obtained with the inhibitors, we subjected mutants deficient in Cyd, Cox and Cox/Cyd to MIMS analysis, first in the absence of inhibitors (Table 1). Dark respiration was reduced in the Δ*cyd* and Δ*cox* mutants and almost abolished in Δ*cox*/*cyd*. Interestingly, light-induced O_2 uptake was significantly higher in both the Δ*cyd* and Δ*cox* mutants compared to the WT, presumably due to up-regulation of the other RTO pathway (Fig. 2, Table 1). In line with this, Δ*cox*/*cyd* demonstrated nearly similar light-induced O_2 uptake rates to the WT. Likewise, the total light O_2 uptake was also increased in the single mutants, whereas substantial decrease was observed in Δ*cox*/*cyd* compared to the WT. All RTO-deficient mutants demonstrated similar gross and net O_2 production rates to WT cells (Table 1).

In the presence of DBMIB, the rate of dark O_2 uptake was similar between all strains, whereas the light-induced O_2 uptake was completely inhibited in the Δ*cyd* and Δ*cox*/*cyd* mutants, and also significantly reduced in Δ*cox* (Table 1). Overall, this resulted in a greatly reduced rate of total O_2 uptake under light in Δ*cyd* and Δ*cox*/*cyd*, but not in Δ*cox*. DBMIB also caused a drastic reduction in gross O_2 production in Δ*cyd* and Δ*cox*/*cyd*, so that the rates were equal to the total O_2 uptake rates under light, as observed in WT cells. The addition of HQNO to the DBMIB-treated cells did not alter O_2 uptake rates in Δ*cyd* cells. Similar to the WT, the addition of DBMIB and HQNO to Δ*cox* eliminated light-induced O_2 uptake detected in the presence of DBMIB only. These results correlated with the experiments performed on WT cells with inhibitors and confirmed that Cyd is responsible for the majority of light-induced O_2 uptake in the presence of DBMIB.

The impact of RTOs under fluctuating light conditions

It was recently reported that the Δ*flv1*/*3* mutant exposed to fluctuating light (FL) conditions exhibited extensive damage to PS I, a drastic decrease in net photosynthesis and to the KCN-sensitive component of light-induced O_2 uptake (Allahverdiyeva et al., 2013). To address a possible role of Cyd in light-induced O_2 uptake under FL conditions, MIMS analysis was undertaken in WT and Δ*flv1*/*3* cells incubated under the FL 20/500 regime (20 μmol photons m^{-2} s^{-1} background light interrupted by 30 s pulses of 500 μmol photons m^{-2} s^{-1} light every 5 min) for 3 days. The samples were analyzed either in the absence (control) or in the presence of HQNO, following illumination of the cells with strong white light of 400 μmol photons m^{-2} s^{-1}. In WT cells, the addition of HQNO did not significantly affect the light-induced fraction of O_2 uptake (Fig. 3). Interestingly, the addition of HQNO to Δ*flv1*/*3* cells acclimated to FL conditions resulted in an 86% inhibition of the light-induced O_2 uptake rate, indicating a significant contribution of Cyd to O_2 uptake in the light.

To investigate further a possible role for Cyd and Cox in the acclimation of cyanobacterial cells to fluctuating light, the growth of RTO-deficient mutants was monitored under the FL 20/500 regime for several days. No significant differences were observed in the growth of the mutants, compared to WT cells (Fig. 4A). Previously it has been shown and we have also confirmed that the Δ*cox*/*cyd* double mutant is not viable when subjected to a 12 h dark/12 h high light (150 μmol photons m^{-2} s^{-1}) square-wave cycle regime (Lea-Smith et

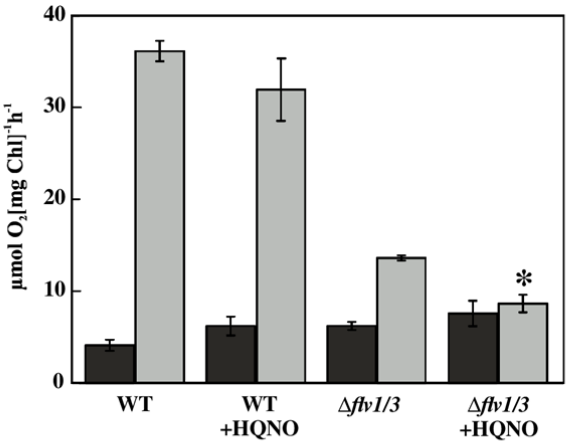

Figure 3. The rates of total O_2 uptake in darkness (black bars) and under the light (grey bars) in the WT and Δ*flv1/3* acclimated for 3 days to the fluctuating light FL 20/500 regime (20 µmol photons m^{-2} s^{-1} background light interrupted by 30-s pulses of 500 µmol photons m^{-2} s^{-1} light every 5 min). Measurements were performed using MIMS on cells incubated in darkness for 5 min and then illuminated with a strong white light (400 µmol photons m^{-2} s^{-1}) for 5 min either in the absence (control) or in the presence of HQNO. Mean ± SD, n=3, asterisk indicates statistically significant difference between measurement with HQNO compared to control samples ($P<0.05$).

al., 2013, Fig. S3A). Interestingly, when the duration of alternating dark and high-light phases was decreased to 5 min (5 min dark/5 min high-light 200 µmol photons m^{-2} s^{-1}) the Δ*cox*/*cyd* mutant survived (Fig. 4B). However, the growth of this strain and of the Δ*cox* mutant was slower after 7 days, compared to the WT and Δ*cyd*.

Gas-exchange analysis of the PS I-less mutant

A possible role of RTOs in light-stimulated electron transfer to O_2 in the PS I-less mutant (Shen et al., 1993), which is lacking functional PS I, was also studied by MIMS gas-exchange analysis. The ΔPSI cells demonstrated strong light-induced O_2 uptake which was insensitive to HQNO. However, this could be completely abolished by the addition of KCN (Fig. 5). These results indicated that in the cells lacking functional PS I, it is not Cyd but Cox which is shuttling electrons to O_2 during sudden, strong illumination.

Response of photosynthesis in RTO-deficient mutants to increasing light intensities

To characterize the impact of RTOs on photosynthetic electron transfer, "rapid light curves", representing the response of photosynthetic parameters to gradually increasing light intensities, were recorded (Fig. 6). During the experiment the cells were illuminated with actinic light of different intensities for 60 s and a saturating pulse was applied at the end of each light period. The effective yield of PS II, Y(II), and the donor side limitation

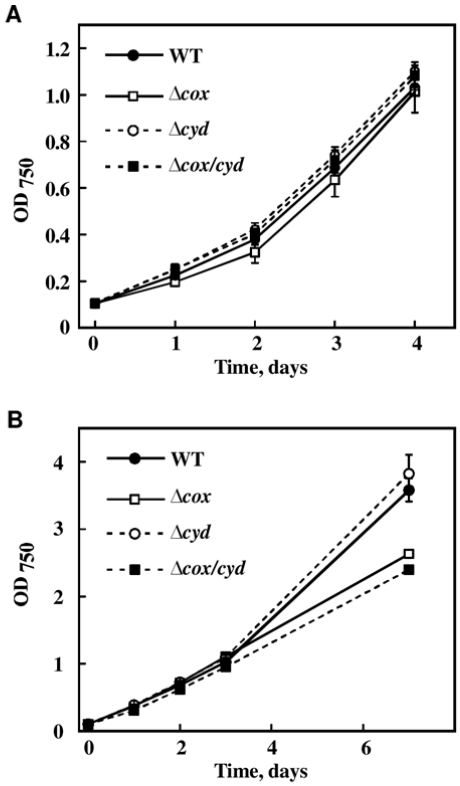

Figure 4. The growth of *Synechocystis* WT and RTO-deficient mutants under: (A) fluctuating light, FL 20/500 (20 μmol photons $m^{-2} s^{-1}$ background light, interrupted every 5 min with 30 s high light pulses of 500 μmol photons $m^{-2} s^{-1}$); (B) 5 min dark / 5 min high light (200 μmol photons $m^{-2} s^{-1}$) square-wave cycles. Mean ± SD, n=3.

of PS I, Y(ND), were specifically addressed to monitor the status of the intersystem electron transfer chain. The Δ*cox* mutant was similar to the WT in the dynamics of Y(II), whilst Δ*cyd* and Δ*cox*/*cyd* demonstrated a decrease of Y(II) under increasing light intensities (Fig. 6A). In Δ*cyd* cells a decrease in PS II yield was observed under light intensities ranging from 57 to 220 μmol photons $m^{-2} s^{-1}$. The Δ*cox*/*cyd* double mutant already displayed a decrease in PS II yield at the lower light intensities, starting at 10 μmol photons $m^{-2} s^{-1}$ (Fig. 6A).

The dynamics of the donor side limitation of PS I, Y(ND), was again similar between WT and Δ*cox* cells; Y(ND) rose gradually as the light intensity increased (Fig. 6B). Interestingly, in Δ*cyd* and Δ*cox*/*cyd* mutant cells, Y(ND) rose faster than in the WT and significantly exceeded the WT values at 58 μmol photons $m^{-2} s^{-1}$ (Fig. 6B). However under higher light intensities, starting from 220 μmol photons $m^{-2} s^{-1}$, there was a slight but statistically significant difference ($P<0.05$) in Y(ND) between Δ*cyd* and Δ*cox*/*cyd*. This result suggests that under high light the reduced electron flow to P700 in the Δ*cyd* mutant

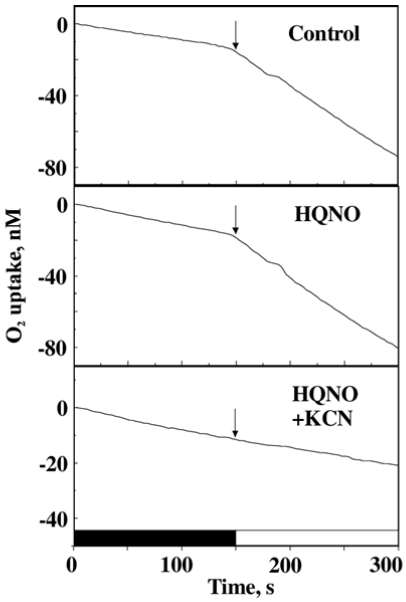

Figure 5. MIMS analysis of O_2 uptake by PS I-less mutant cells in the absence (control) and in the presence of HQNO and HQNO+KCN. O_2 uptake was monitored for 5 min in darkness and 5 min under the light intensity of 150 μmol photons m^{-2} s^{-1}. Arrows indicate the beginning of illumination. The slope of the curves does not provide a precise quantitative measure of the rate of O_2 consumption until it is corrected for the isotopic ratio ($^{16}O/^{18}O$).

was presumably due to increased competition for electrons between PS I and Cox. No significant difference between WT and RTO-mutants was observed in acceptor side limitation of PS I, Y(NA) (Fig. S4).

To investigate whether sensitivity of the Cyd-deficient mutants to increasing light intensities would affect the growth of cells under high light, we grew highly diluted cultures of the WT and RTO-deficient mutants at a continuous light intensity of 500 μmol photons m^{-2} s^{-1} (Fig. S3B). None of the mutants exhibited light-sensitivity under these conditions and all cultures reached a similar OD_{750} after 2 days of growth.

Analysis of the PQ pool redox status in RTO-mutants in darkness

Next we studied the PQ pool redox state in RTO-deficient mutants in darkness and under far-red (FR) illumination using Chl fluorescence analysis (Fig. 7). The dark-adapted cells of WT, Δ*cox* and Δ*cyd* demonstrated similar F_0 levels of minimal fluorescence in the dark, whereas Δ*cox*/*cyd* cells had a significantly higher F_0 level (Table S1). Next, a saturating pulse was applied to the cells to obtain the maximum fluorescence signal in darkness (F_M^D). All strains demonstrated similar F_M^D values (Table S1). The double mutant retained a higher level of fluorescence in the dark compared to the WT, whilst the Δ*cox* cells

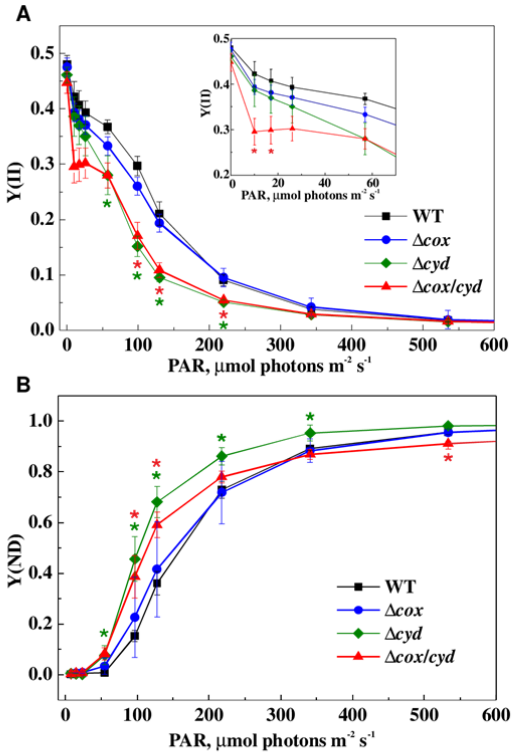

Figure 6. Rapid light curves of the WT and RTO-deficient mutants: (A) PS II yield, Y(II); (B) Donor side limitation of PS I, Y(ND). Mean ± SD, n=3. Asterisks indicate a statistically significant difference compared to the WT ($P<0.05$).

exhibited a slower relaxation of saturating pulse-induced fluorescence during the subsequent dark period (Fig. 7).

Due to the high flow of electrons to the electron transport chain from respiratory complexes, cyanobacterial cells are usually in State II during dark periods (Mullineaux and Allen, 1986) and therefore demonstrate low F_M^D values. In order to induce a State II to State I transition cells were then exposed to FR for 8 s to preferentially excite PS I and facilitate oxidation of the PQ pool. FR application did not affect the fluorescence level in the WT and single mutants; however, it resulted in a sudden drop of fluorescence in the Δ*cox*/*cyd* double mutant, to a level just slightly above those of WT and single mutant cells (Fig. 7). A FR-mediated decrease of fluorescence suggested a highly reduced PQ pool in Δ*cox*/*cyd* cells in darkness, which is in agreement with an earlier study by Howitt *et al* (2001). When a saturating pulse was applied over a FR background, all strains demonstrated an increased F_M^{FR} (Fig. 7, Table S1). Afterwards the relaxation of fluorescence was again recorded in darkness. The fluorescence levels of WT and Δ*cyd* cells dropped down to a value similar to their initial F_0 levels. The fluorescence signal of

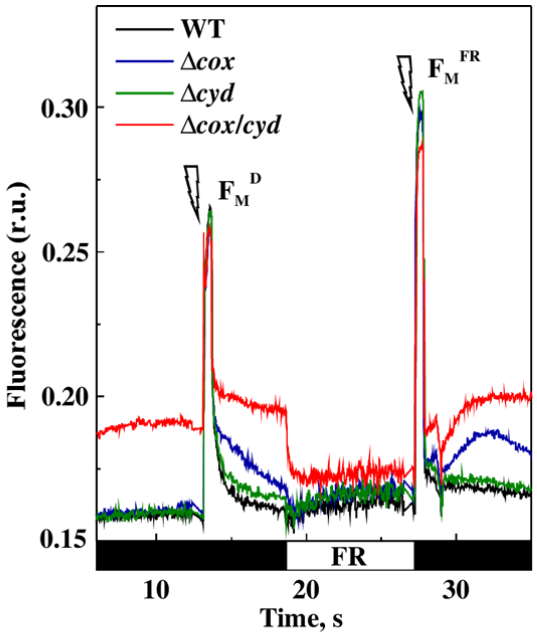

Figure 7. Fluorescence analysis of the WT and RTO-deficient mutant cells. Fluorescence was recorded in darkness (minimal fluorescence, F_0, black bars on the timescale) and under far-red light (FR). Saturating pulses indicated by flashes were fired to monitor maximum fluorescence level in the dark (F_M^D) and under the FR background (F_M^{FR}). The values are provided in Table S1. Samples were adjusted to a Chl concentration of 15 μg mL^{-1} and dark-adapted for 10 min before the measurements. Results of one representative experiment of three independent experiments are shown.

the Δ*cox*/*cyd* mutant immediately returned to its initial higher level, demonstrating rapid reduction of the PQ pool in darkness. The Δ*cox* cells demonstrated only a transient increase and subsequent relaxation of the fluorescence level after the termination of FR illumination.

Characterization of PS II functional status in RTO-mutants

To analyze in detail the functional status of PS II in the RTO mutants, the maximum quantum yield of PS II (F_V/F_M) was first measured with the Dual-PAM fluorometer in the presence of DCMU. The values did not differ significantly between the WT and mutants (Table S1). This is in line with the MIMS data showing nearly similar gross O_2 production in all studied RTO-deficient mutants compared to the WT (Table 1).

Next, the status of the PS II acceptor and donor sides in these strains was precisely addressed by comparing the relaxation kinetics of the flash-induced fluorescence yield. Following a single-turnover flash, relaxation of the variable fluorescence yield in darkness

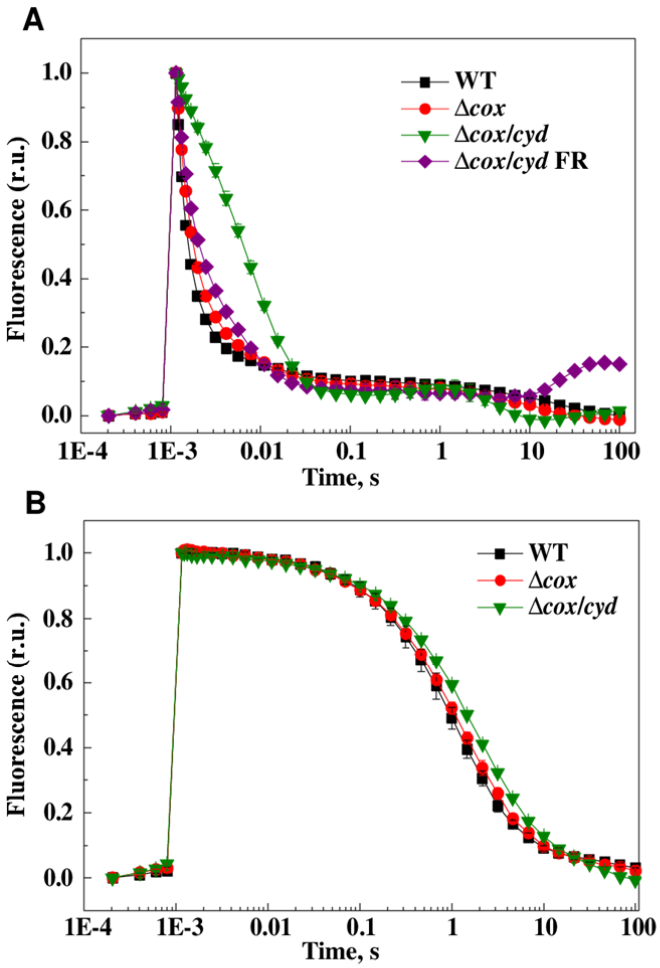

Figure 8. Relaxation of the flash-induced fluorescence yield in darkness. Q_A^- re-oxidation was monitored: (A) from the dark-adapted WT (black squares), Δ*cox* (red circles), Δ*cox/cyd* (green diamonds) and Δ*cox/cyd* (purple diamonds) cells pre-illuminated with far-red light for 30 s; (B) in the presence of 20 μM DCMU. Mean ± SD, n=3. The F_0 and F_M values were normalized to 0 and 1, respectively, to facilitate comparison of the kinetics.

reflects the Q_A^- re-oxidation via forward Q_A-to-Q_B electron transfer and back recombination with $S_{2/3}$ states of the water-oxidizing complex of PS II. The fluorescence relaxation kinetics were comparable for WT and Δ*cyd* cells (Fig. S5A), whilst Δ*cox* showed a slower fluorescence decay and the Δ*cox*/*cyd* mutant demonstrated a drastically slower decay (Fig. 8A). These data indicated modified electron transfer at the PS II acceptor side in Δ*cox*, which is exacerbated further in the Δ*cox*/*cyd* mutant cells. Interestingly, the fluorescence relaxation curve of Δ*cox*/*cyd* displayed a slight "wave phenomenon", showing a dip at the time point of approximately 50 ms and a transient rise

of fluorescence at about 1 s after the flash. Deák et al. have recently observed similar kinetics of fluorescence relaxation in *Synechocystis* cells when the electron flow to O_2 was inhibited under anoxic conditions (Deák et al., 2014). This was due to transient oxidation of the highly reduced PQ pool by PS I, followed by its re-reduction from cytosolic components via the NDH-1 complex.

In order to clarify whether the slower relaxation kinetics of the Δ*cox* and Δ*cox*/*cyd* mutants were due to a reduced PQ pool, or to structural modifications in the PS II complex, strong FR illumination was applied to cells just before fluorescence measurements. Pre-illumination of the Δ*cox*/*cyd* cells with FR, preferentially exciting PS I and thus oxidizing the PQ pool, significantly accelerated the fluorescence decay, bringing the curve closer to that of Δ*cox* cells (Fig. 8A). However, after 10 s of darkness the fluorescence level of the Δ*cox*/*cyd* cells again started to increase. These results strongly suggest that a slowdown of the Q_A re-oxidation rate in Δ*cox*/*cyd* was predominantly due to a highly reduced PQ pool in darkness. However, FR illumination did not significantly affect the fluorescence relaxation kinetics of the Δ*cox* cells (Fig. S5B).

In the presence of DCMU, which blocks electron transfer at the Q_B site, Q_A^- re-oxidation occurs via charge recombination with the donor side components, mostly the S_2 state of the water oxidizing complex (Vass et al., 1999). Interestingly, in the presence of DCMU, Δ*cox*/*cyd* still demonstrated slightly slower fluorescence relaxation, compared to the WT, likely indicating accumulation of PS II centers with a modified donor side in the mutant cells. The Δ*cox* and Δ*cyd* cells showed a similar relaxation kinetics profile to the WT (Fig. 8B).

The P700 redox state in the RTO-deficient mutants

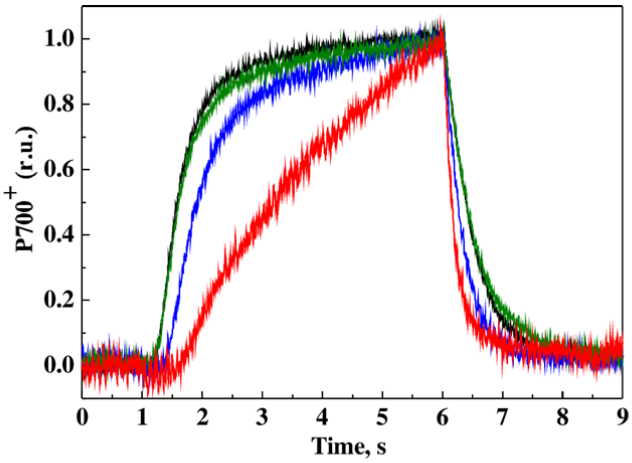

Figure 9. P700 oxido-reduction. P700 oxidation and re-reduction in the WT and mutant cells illuminated with strong far-red light for 5 s. WT (black); Δ*cox* (blue); Δ*cyd* (green); Δ*cox*/*cyd* (red). Curves were normalized to the same amplitude to facilitate comparison of the kinetics. Results of one representative experiment of three independent experiments are shown.

The redox state of P700 was monitored during dark-light-dark transitions by the application of strong FR light (Fig. 9). The kinetics of P700 oxidation and re-reduction were similar between WT and Δ*cyd* cells. The Δ*cox* mutant demonstrated a small lag-phase during oxidation of P700 and faster re-reduction compared to the WT. Drastically slower oxidation and faster re-reduction was recorded for the Δ*cox*/*cyd* mutant, as compared to the WT and single mutants (Fig. 9). This is in line with the fluorescence analysis results, implying a highly reduced PQ pool in Δ*cox*/*cyd* cells in darkness. However, the maximum amount of oxidizable P700 (P_M) did not differ significantly between the WT and RTO-deficient mutants (Table S1).

The PS II/PS I ratio in the RTO-deficient mutants

In order to determine whether the modified redox state of the PQ pool observed in the double mutant during dark-to-light transitions affected energy transfer between photosystems, the 77K fluorescence emission spectra of the WT and RTO-deficient mutants was analyzed. Spectra of mutant cells excited with either 440-nm (Chl excitation) or 580-nm (phycobilisome excitation) light did not differ from the WT spectra (Fig. S6), suggesting the absence of significant changes in the PS II/PS I ratio and in energy transfer from phycobilisomes to the reaction centers of photosystems. In addition, total protein fractions were isolated from the cells grown under continuous light (50 μmol photons m^{-2} s^{-1}) and probed with a range of antibodies. The amount of PsaB and PsbA (D1), proteins in

445 the reaction centers of PS I and PS II, respectively, were similar between all strains (Fig.
446 S7). Likewise amounts of the ATP synthase β subunit and Flv2, Flv3 and Flv4 were
447 similar between all strains.
448
449

DISCUSSION

The intersystem electron transport chain of photosynthetic organisms plays an important role in regulation of the photosynthetic apparatus. The Cyt b_6f complex in higher plants is known to act in photosynthetic control, regulating electron flow to PS I (Nishio and Whitmarsh, 1993; Joliot and Johnson, 2011; Suorsa et al., 2013). In *Synechocystis*, the presence of thylakoid membrane-localized terminal oxidases, Cyd and Cox, strongly suggests that RTOs may regulate the intersystem electron transport, not only under dark conditions, but also during light periods. In *Synechocystis*, the total O_2 uptake in the light could consist of two components: the "respiratory component" and the light-induced component. The "respiratory component" can be detected in darkness but could also contribute to the total O_2 uptake observed under light, whereas the light-induced component can only be monitored upon the application of light and is estimated by subtracting the "respiratory component" from total O_2 uptake under light. Shifting cells from darkness to dim light is known to inhibit O_2 uptake by RTOs (Kok effect), likely because of higher affinity of PS I for electrons from Pc and Cyt c_6 (Kok, 1949). However, accurately determining the contribution of specific respiratory RTOs to the total O_2 uptake under moderate or high light is a challenge, mainly because it is not known how their relative activity changes under different conditions.

Cyd contributes to the redox poise of the PQ pool under light

It was generally accepted that addition of DBMIB should maintain a reduced PQ pool during periods of illumination by blocking electron transport at the site of Cyt b_6f (Trebst et al., 1970; Yan et al., 2006). Therefore, in numerous studies, DCMU or DBMIB was added to cyanobacterial cells in order to simulate either an oxidized or reduced redox state of the PQ pool (Hihara et al., 2003; Huang et al., 2003). However, recent data obtained via HPLC demonstrated that in WT *Synechocystis* cells the PQ pool is not as highly reduced during illumination in the presence of DBMIB as previously thought (Schuurmans et al., 2014). Here we demonstrate that, following inhibition of linear electron transport with DBMIB, WT cells of *Synechocystis* are capable of light-induced O_2 uptake, indicating the presence of an alternative electron exit route from the PQ pool to O_2 in the light (Fig. 2). Observed stimulation of O_2 reduction in the light was completely missing after the addition of HQNO to DBMIB treated WT and Δ*cox* cells as well as in the Δ*cyd* and Δ*cox*/*cyd* cells subjected to DBMIB only (Fig. 2, Table 1). Thus, Cyd contributes to the light-induced O_2 uptake observed in the WT when linear electron transport is limited.

Earlier studies already suggested that Cyd is involved in oxidation of the PQ pool (Schneider et al., 2001; Berry et al., 2002; Schneider et al., 2004). However, those studies were based on an indirect fluorescence method. Through application of the $^{18}O_2$ isotope and the MIMS technique, we could directly demonstrate the O_2 uptake activity of Cyd (Fig. 2) and also confirmed that Cyd accepts electrons directly from the PQ pool, since the addition of DCBQ eliminated Cyd-mediated light-induced O_2 uptake (Fig. S2A). In the presence of DBMIB, the rates of total O_2 uptake in the light were similar to the rates of gross O_2 production by PS II. Therefore the rate of net photosynthesis was close to zero in the WT and single mutants (Table 1). Importantly, the gross O_2 production rates were about four times higher in the WT and Δ*cox* cells compared to the Δ*cyd* and Δ*cox*/*cyd* suggesting that the quinol-oxidizing activity of Cyd contributes to alleviation of PS II acceptor side limitation and facilitates gross O_2 production in the presence of DBMIB. This is corroborated by earlier reports which demonstrated an increased level of Cyd associated with impairment of the Cyt b_6f complex in the mutants lacking LepB1 and PetC1 (Zhang et al., 2013; Tsunoyama et al., 2009).

A decrease of the effective PS II yield in the Δ*cyd* and Δ*cox/cyd* mutant cells upon a sudden increase in light intensity indicates, that in the absence of Cyd, electrons accumulate in the PQ pool and affect the Y(II) levels (Fig. 6A). These data also demonstrate that PQH_2 oxidation by Cyt b_6f is the rate-limiting step in the linear electron transport under sub-optimal conditions. Conservation of the PQH_2 oxidizing terminal oxidases, either Cyd, ARTO or PTOX, in all sequenced cyanobacteria which are potentially exposed to high light, further emphasizes the importance of an alternative electron exit pathway to that provided by Cyt b_6f (Lea-Smith et al., 2013). An example occurs in the marine cyanobacterium, *Synechococcus* WH8102, which exhibits a significant flow of electrons to O_2, likely via PTOX, and is caused by the highly reduced state of the PQ pool due to the shortage of Cyt b_6f and PS I in an iron-limited environment (Bailey et al., 2008). Moreover, Δ*cyd* develops high PS I donor side limitation more rapidly under elevated light intensities (Fig. 6B), due to up-regulated Cox activity, as is shown by the increased light-induced O_2 uptake rate in this strain (Table 1). Previous studies also suggest that the activity of RTOs in the light might be regulated by the redox

state of Pc and Cyt *c* (in the case of Cox) and, plausibly, by the redox state of the PQ pool (in the case of Cyd, PTOX and possibly ARTO) (Ardelean and Peschek, 2011).

Interplay between Cyd and flavodiiron proteins

It is clear that both Flv1 and Flv3 are responsible for the light-induced O_2 uptake in *Synechocystis* at least during dark to high light transitions (Fig. S1, Helman et al., 2003; Allahverdiyeva et al., 2011). Helman et al. (2005) estimated that in low CO_2-grown cells of Δ*flv3*, RTOs redirect 6% of electrons originating from water splitting to O_2 in the light. Thus, upon application of strong light, the mutant retains the "respiratory component" of O_2 uptake driven by RTOs as an alternative sink for light-driven electrons. In agreement with this, under fluctuating light conditions, where electron transfer chain is drastically inhibited in Δ*flv1*/*3* due to damage to PS I (Allahverdiyeva et al., 2013), the Δ*flv1*/*3* mutant showed an HQNO-sensitive light-induced O_2 uptake (Fig. 3). This is yet another demonstration of Cyd-driven light-induced O_2 uptake when cells are grown under sub-optimal conditions, despite the absence of changes in *cyd* transcript level under FL (Mustila et al., 2016).

It has been previously reported that light-induced O_2 uptake in the Δ*flv1*/*3* cells under FL was functioning at full capacity when cells were exposed to background dim light (20 μmol photons m^{-2} s^{-1}), and that this did not increase further upon the application of high-light pulses. Therefore, Cyd cannot rescue the fatal Δ*flv1*/*3* phenotype (Allahverdiyeva et al., 2013). The unambiguous importance of Flv1 and Flv3 under fluctuating light indicates that they are functioning on a fast time scale downstream of PS I, and have a higher capacity as an electron sink under these conditions, compared to the RTOs. In part this could be due to the soluble nature of Flv1 and Flv3, which would facilitate rapid association with NADPH and allow large amounts of protein to accumulate in the cytosol. In contrast, RTOs are membrane-localized and may be limited in number, due to the highly crowded nature of the thylakoid membrane. Following rapid light changes, a time consuming redistribution of protein complexes occurs within the membrane in order to facilitate efficient electron transfer (Mullineaux, 2014b; Liu et al., 2012).

Cox is mostly active in dark respiration, and can be substituted by Cyd under light conditions

549 The contribution of Cyd to dark respiration seems to be minor, since the redox state of the
550 PQ pool in Δ*cyd* cells was not affected in darkness, as confirmed via P700 oxido-reduction
551 (Fig. 9), Q_A^- re-oxidation kinetics (Fig. 8, Fig. S5), and fluorescence analysis (Fig. 7).
552 However, the presence of Cyd was beneficial in Δ*cox* cells under light, since the Q_A^- re-
553 oxidation and the P700 oxido-reduction kinetics differed significantly between Δ*cox* and
554 Δ*cox*/*cyd* cells (Fig. 8, Fig. 9). In contrast to Δ*cyd*, deletion of Cox drastically decreased
555 the rate of dark respiration (Table 1; Howitt and Vermaas, 1998; Pils et al., 1997; Pils and
556 Schmetterer, 2001) and had a prominent effect on the redox state of the PQ pool in
557 darkness (Fig. 7, Fig. 8, Fig. 9), but not under illumination (Fig. 6). Therefore, in
558 *Synechocystis,* Cox can be efficiently substituted by Cyd under illumination. Nevertheless,
559 in the PS I-less mutant of *Synechocystis*, Cox instead of Cyd was the main RTO shuttling
560 electrons to O_2 in the light (Fig. 5). Since Cox is required for chemoheterotrophic growth
561 of *Synechocystis* (Pills et al., 1997) and the PS I-less mutant grows in the presence of
562 glucose under a low light intensity of 5 μmol photons m^{-2} s^{-1}, it is highly possible that Cox
563 is the main thylakoid-localized RTO in this mutant. However, since the PS I-less mutant is
564 highly sensitive to light (Shen et al., 1993), the contribution of Cox as an electron shuttle
565 to O_2 is likely to be less efficient compared with PSI activity or this could be a transient
566 phenomenon. It is possible that under specific conditions Cox also produces ROS via a
567 mechanism similar to PTOX in plants (Heyno et al., 2009; Feilke et al. 2014; Yu et al.
568 2014), thereby generating oxidative damage to the cells. On the other hand, rapid light
569 curve analysis demonstrated a slight but significant difference in Y(ND) values between
570 Δ*cyd* and Δ*cox*/*cyd* cells under higher light intensities indicating competition between PS I
571 and Cox for electrons in the Δ*cyd* mutant (Fig 6B). Thus, both Cyd and Cox have a role in
572 regulating the amount of electrons arriving to PS I in the light, although Cox activity only
573 increases only in the absence of Cyd.
574
575 **The role of RTOs in dark/light transitions**
576 Despite strong evidence for thylakoid-based RTOs regulating photosynthetic electron
577 flow, deletion mutants do not demonstrate a strong photoautotrophic growth phenotype
578 under continuous moderate light (Howitt and Vermaas, 1998; Lea-Smith et al., 2013), high
579 light (Fig. S3B, Lea-Smith et al., 2013) and fluctuating light intensity regimes (Fig. 4A).
580 Thus, it is likely that when the Flv1/3 complex is functioning properly under illumination,
581 RTOs are not essential. However, during periods of darkness, only RTOs can oxidize the

582 PQ pool, as demonstrated by the Δ*cox*/*cyd* mutant having a drastically slower oxidation
583 and faster re-reduction rate of P700, and slower Q_A^- re-oxidation kinetics in the dark (Fig.
584 7, Fig. 8, Fig. 9). Importantly, the PQ pool in the double mutant could be immediately
585 oxidized by the application of strong FR light (Fig. 7, Fig. 8) but not by the application of
586 low light. The latter result could be concluded from a decreased Y(II) in the light curve
587 analysis at 10-30 μmol photons m^{-2} s^{-1} light intensity (Fig. 6A). However, in the same
588 experiment under moderate and high light intensities, Δ*cox*/*cyd* behaved similarly to the
589 Δ*cyd* cells.
590
591 Either Cox or Cyd is required for survival of cells under 12 h high light/12 h dark square-
592 wave cycles (Fig. S3A, Lea-Smith et al., 2013) but interestingly not under 12 h high
593 light/12 h dark sinusoidal-wave cycles (Lea-Smith et al., 2013) or 5 min high light/5 min
594 dark square-wave cycles (Fig. 4B). Therefore, the importance of RTOs seems to depend on
595 both the length of the dark and light periods and the amount of photodamage occurring
596 during the light period. Indeed, significant ROS production and inactivation of the PS II
597 complex was observed in the double mutant subjected to 12 h high light/12 h dark square-
598 wave cycles only at the end of a long dark period, possibly due to an insufficient amount
599 of ATP for PS II repair and an over-reduced PQ pool (Lea-Smith et al., 2013). Under 12 h
600 high light/12 h dark sinusoidal-wave cycles, (i) cells are not subjected to rapid high light
601 exposure, reducing damage to PS II, moreover (ii) damaged PS II centers have a
602 possibility for efficient repair during a low light phase before a dark period, therefore the
603 cells have a reduced energy requirements for repair, which can be substituted by
604 alternatives to dark respiration, most likely fermentation.
605
606 Under short dark/light periods (Fig. 4B) the cells may be able to oxidize the PQ pool
607 regularly, thus generating ATP and reducing power which can be used in darkness,
608 although not as efficiently as the WT, since growth of the Δ*cox* and Δ*cox*/*cyd* mutants was
609 reduced after 7 days.
610
611 **CONCLUSION**
612 Through the use of well-defined mutants and inhibitors combined with MIMS gas-
613 exchange analysis, we show the subtle effects of loss of RTO complexes on each part of
614 the photosynthetic electron transfer chain. Importantly, RTO-mediated respiratory O_2

uptake can continue at a similar rate upon high light illumination, thus contributing to oxidation of the PQ pool. Cox is the most important RTO in dark respiration, but also competes with PS I for electrons, functioning as a regulator of the electron flow to this photosystem under high light. Under illumination, Cyd is the major RTO oxidizing PQH_2. However, Cyd only up-regulates O_2 photoreduction under certain conditions, specifically when Flv1 and Flv3 protein activity is insufficient to prevent linear electron transport blockage at the level of Cyt b_6f or PS I. Flv1 and Flv3 proteins are not involved in dark respiration but are responsible for the majority of the light-induced O_2 uptake component. Thus both RTOs and Flv1/3 pathways play an important role in alleviation of excess electrons using O_2 as a terminal acceptor under illumination: RTOs continue to function in the light, although operating on slower time ranges and on limited scale, whereas Flv1/3 responds rapidly as a light-induced component and with greater capacity.

MATERIALS AND METHODS

Strains and Culture Conditions

The strains used in this study included *Synechocystis* sp. PCC 6803 (WT), mutants lacking respiratory terminal oxidases: Δ*cyd*, Δ*cox*, Δ*cox*/*cyd* (all described previously in Lea-Smith et al., 2013); mutant deficient in flavodiiron proteins: Δ*flv1*/*flv3* (Allahverdiyeva et al., 2011) and the PS I-less mutant (Shen et al., 1993). Cells were maintained in BG11 medium buffered with 10mM N-[Tris(hydroxymethyl)methyl]-2-aminoethanesulfonic acid (TES-KOH, pH 8.2) under continuous illumination of 50 μmol photons m^{-2} s^{-1} (PAR), 3% CO_2, 30 °C with gentle agitation (120 rpm). For all physiological experiments cells were inoculated to OD_{750nm}=0.5-0.6 and shifted to ambient CO_2 conditions for 3 days before measurements. Experimental cultures were cultivated in AlgaeTron AG130 growth chambers (PSI Instruments, Czech) under continuous illumination of 50 μmol photons m^{-2} s^{-1} (provided by cool-white LED), unless mentioned otherwise. For the high light growth experiments, a dilution series of cells starting from OD_{750}=0.1 were subjected to a light intensity of 500 μmol photons m^{-2} s^{-1}. For the MIMS measurements of fluctuating light-treated cells, cultures at an OD_{750}=0.5-0.6 were shifted to a light regime with a background light of 20 μmol photons m^{-2} s^{-1} interrupted by 30 s pulses of 500 μmol photons m^{-2} s^{-1} light every 5 min (FL 20/500). For the growth experiments under fluctuating light

conditions, cells were subjected to FL 20/500 or a 5 min dark/5 min 200 μmol photons m^{-2} s^{-1} light regime starting from an OD_{750}=0.1. For all activity measurements, cells were harvested and resuspended in fresh BG11 medium at the desired Chl concentration and acclimated for 1 h under respective growth conditions before the measurements. The PS I-less mutant was grown in the presence of 5 mM glucose at a light intensity of 5 μmol photons m^{-2} s^{-1}.

Membrane Inlet Mass Spectrometry (MIMS)

Online measurements of $^{16}O_2$ (mass 32) production and $^{18}O_2$ (mass 36) consumption were monitored using mass spectrometry (model Prima PRO, Thermo Scientific). The membrane inlet system consists of a thermo-regulated DW1 oxygen electrode chamber, which is connected to the vacuum line of the mass spectrometer via a gas-permeable thin Teflon membrane (1 mil stretch membrane, YSI Inc, Ohio, USA), which seals the bottom of the chamber. For analyses, 1.5 ml of cell suspension at a Chl concentration of 15 μg mL^{-1} was placed into the measuring chamber and stirred continuously. Gases dissolved in the medium diffuse through the Teflon membrane to the ion source of the mass spectrometer. Prior to the measurement, $^{18}O_2$ (isotope purity > 98%; CK Gas Products Ltd) was injected by bubbling at the top of the suspension until the concentrations of $^{16}O_2$ and $^{18}O_2$ were equal. Then samples were measured for 5 min in darkness to record O_2 consumption caused by respiration. Following this period, actinic light (400 μmol photons m^{-2} s^{-1}; 150 μmol photons m^{-2} s^{-1} in the case of the PS I-less mutant) was applied via a 150 Watt, 21 V, EKE quartz halogen-powered fiber optic illuminator (Fiber-Lite DC-950, Dolan-Jenner, MA, USA). Gas-exchange kinetics and rates were determined according to Beckmann et al. (2009). The final concentration of inhibitors and electron acceptors used in MIMS experiments was 25 μM DBMIB, 50 μM HQNO, 0.5 mM DCBQ and 1 mM KCN. All the measurements were performed in the presence of 1 mM $NaHCO_3$.

Protein Isolation, Electrophoresis, and Immunodetection

Total protein extracts of *Synechocystis* cells were isolated as described in Zhang et al. (2009). Proteins were separated by 12% (w/v) SDS-PAGE containing 6 M urea, transferred to a PVDF membrane (Immobilon-P, Millipore) and analyzed with the protein-specific antibodies.

Fluorescence measurements

The Chl fluorescence from intact cells was recorded with a pulse amplitude modulated fluorometer Dual-PAM-100 (Walz, Germany). Prior to measurements, cell suspensions at a Chl concentration of 15 μg mL^{-1} were dark-adapted for 10 min. Saturating pulses of 5,000 μmol photons m^{-2} s^{-1} (300 ms) and strong far-red light (720 nm, 75 W m^{-2}) were applied to samples when required. The maximum quantum yield of PS II was calculated as $(F_M-F_0)/F_M = F_V/F_M$, and measured in the presence of 20 μM DCMU from dark-adapted cells upon the application of red actinic light of 200 μmol photons m^{-2} s^{-1} for 1 min.

The kinetics of the Chl fluorescence decay after a single-turnover saturating flash were monitored using a fluorometer FL 3500 (PSI Instruments) according to Vass et al. (1999). Cells were adjusted to a Chl concentration of 7.5 μg mL^{-1} and dark-adapted for 5 min before measurements. When indicated, measurements were performed in the presence of 20 μM DCMU. In some experiments cells were illuminated for 30 s with a strong far-red light before application of the flash.

The fluorescence emission spectra at 77K were measured from intact cells using a USB4000-FL-450 (Ocean Optics) spectrofluorometer. Samples were removed from cultures, adjusted to a Chl concentration of 7.5 μg mL^{-1}, rapidly frozen in liquid nitrogen and excited with 580 nm or 440 nm light generated with interference filters 10 nm in width.

P700 Oxidation and Re-reduction

Oxidation and re-reduction of P700 was monitored using a Dual-PAM-100 (Walz). Cell suspensions at a Chl concentration of 20 μg mL^{-1} were dark-adapted for 2 min before measurements. For P700 oxidation, cells were illuminated with strong far-red light (720 nm, 75 W m^{-2}) for 5 s and the subsequent re-reduction was recorded in darkness.

Light Curves

Rapid light curves were measured without dark adaptation of the cells using standard protocols programmed into a Dual-PAM-100 (Walz) with the 60 s illumination periods gradually increasing in light intensity. At the end of each light period a saturating pulse was applied to monitor the photosynthetic parameters. The effective yield of PS II, Y(II),

was calculated as (F_M'-F_S)/F_M'. The Y(ND), non-photochemical quantum yield of PS I caused by the donor side limitation, was calculated as (P/P_M). The Y(NA), acceptor side limitation of PS I, was calculated as [(P_M - P_M´) / P_M].

Acknowledgments: We are grateful to Dr. W. Vermaas for sharing the PS I-less mutant.

Table 1. O_2 exchange rates of the WT and mutant cells. Rates are in µmol O_2 [mg Chl]$^{-1}$ h^{-1}. Mean ± SD, n=3-5. Asterisks indicate a statistically significant difference compared to the WT (P<0.05).

Gas-exchange conditions			WT	Δ*cyd*	Δ*cox*	Δ*cox*/*cyd*
Control	O_2 uptake	Dark	8.3±1.2	5.1±0.8*	3.5±0.5*	0.3±0.2*
		Light-induced	26.3±6.9	35.3±8.3*	38.4±5.5*	24.7±3.0
		Total Light	34.6±6.7	40.5±7.5	41.5±5.1*	24.9±3.0
	O_2 production	Gross	193.3±20.1	190.7±26.4	190.25±18.1	184.9±21.5
		Net	158.6±19.3	150.3±19.2	148.7±15.1	159.6±22.5
DBMIB	O_2 uptake	Dark	10.1±1.5	13.1±1.3	12.8±3.1	9.3±1.3
		Light-induced	11.6±2.3	N/A	7.9±0.6 *	N/A
		Total Light	21.5±2.8	7.0±0.8*	20.7±2.5	7.7±1.9*
	O_2 production	Gross	24.2±3.1	5.5±1.3*	19.8±3.8*	2.75±0.4*
		Net	2.9±0.2	N/A	N/A	N/A
DBMIB+ HQNO	O_2 uptake	Dark	12.9±0.3	11.3±3.5	10.9±3.9	10.2±0.2*
		Light-induced	N/A	N/A	N/A	N/A
		Total Light	12.3±0.6	7.0±1.1	10.8±3.4	9.8±0.5

Figure Legends

Figure 1. Schematic diagram of the thylakoid membrane-localized photosynthetic and respiratory electron transfer chains. Lines indicate electron transport; dotted lines indicate possible but poorly characterized electron transfer and proton pathways. PS II, Photosystem II; Flv2/4, Flavodiiron proteins 2/4; Flv1/3, Flavodiiron proteins 1/3; PQ, plastoquinone; PQH_2, plastoquinol; Cyt b_6f, cytochrome b_6f complex; Pc, plastocyanin; Cyt c_6, cytochrome c_6; PS I, Photosystem I; Fd, ferredoxin; FNR, ferredoxin-$NADP^+$ oxidoreductase; NDH-1, NAD(P)H dehydrogenase-like complex type 1; SDH, succinate

dehydrogenase; NDH-2, NAD(P)H dehydrogenase type 2; Cyd, cytochrome *bd* quinol oxidase; Cox, cytochrome *c* oxidase.

Figure 2. The rates of O_2 exchange in the WT and Δ*cyd* mutant cells incubated in darkness for 5 min and then illuminated with a strong white light (400 μmol photons m^{-2} s^{-1}) for the next 5 min. Black bars and grey bars indicate the rates of total O_2 uptake by cells in darkness and in the light, respectively; white bars indicate the gross O_2 production rate. Measurements were performed either in the absence of inhibitors (control) or in the presence of DBMIB or DBMIB + HQNO. Mean ± SD, n=3-5.

Figure 3. The rates of total O_2 uptake in darkness (black bars) and in the light (grey bars) in the WT and Δ*flv1/3* acclimated for 3 days to a fluctuating light FL 20/500 regime (20 μmol photons m^{-2} s^{-1} background light interrupted by 30 s pulses of 500 μmol photons m^{-2} s^{-1} light every 5 min). Measurements were performed using MIMS on cells incubated in darkness for 5 min and then illuminated with a strong white light (400 μmol photons m^{-2} s^{-1}) for 5 min either in the absence (control) or in the presence of HQNO. Mean ± SD, n=3, asterisks indicates statistically significant difference between measurement with HQNO compared to control samples ($P<0.05$).

Figure 4. The growth of *Synechocystis* WT and RTO-deficient mutants under: (A) fluctuating light, FL 20/500 (20 μmol photons m^{-2} s^{-1} background light, interrupted every 5 min with 30 s high light pulses of 500 μmol photons m^{-2} s^{-1}); (B) 5 min dark / 5 min high light (200 μmol photons m^{-2} s^{-1}) square-wave cycles. Mean ± SD, n=3.

Figure 5. MIMS analysis of O_2 uptake by PS I-less mutant cells in the absence (control) and in the presence of HQNO and HQNO+KCN. O_2 uptake was monitored for 5 min in darkness and 5 min under a light intensity of 150 μmol photons m^{-2} s^{-1}. Arrows indicate the beginning of illumination. The slope of the curves does not provide a precise quantitative measure of the rate of O_2 consumption until it is corrected for the isotopic ratio ($^{16}O/^{18}O$).

Figure 6. Rapid light curves of the WT and RTO-deficient mutants: (A) PS II yield, Y(II); (B) Donor side limitation of PS I, Y(ND). Mean ± SD, n=3. Asterisks indicate a statistically significant difference compared to WT ($P<0.05$).

Figure 7. Fluorescence analysis of the WT and RTO-deficient mutant cells. Fluorescence was recorded in darkness (minimal fluorescence, F_0, black bars on the timescale) and under far-red light (FR). Saturating pulses indicated by flashes were fired to monitor maximum fluorescence level in the dark (F_M^D) and under the FR background (F_M^{FR}). The values are provided in Table S1. Samples were adjusted to a Chl concentration of 15 µg mL^{-1} and dark-adapted for 10 min before the measurements. A representative curve of three independent experiments is shown.

Figure 8. Relaxation of the flash-induced fluorescence yield in darkness. Q_A^- re-oxidation was monitored: (A) from the dark-adapted WT (black squares), Δ*cox* (red circles), Δ*cox/cyd* (green diamonds) and Δ*cox/cyd* (purple diamonds) cells pre-illuminated with far-red light for 30 s; (B) in the presence of 20 µM DCMU. Mean ± SD, n=3. The F_0 and F_M values were normalized to 0 and 1, respectively, to facilitate comparison of the kinetics.

Figure 9. P700 oxido-reduction. P700 oxidation and re-reduction in the WT and mutant cells illuminated with strong far-red light for 5 s. WT (black); Δ*cox* (blue); Δ*cyd* (green); Δ*cox*/*cyd* (red). Curves were normalized to the same amplitude to facilitate comparison of the kinetics. A representative curve of three independent experiments is shown.

Parsed Citations

Abramson J, Riistama S, Larsson G, Jasaitis A, Svensson-Ek M, Laakkonen L, Puustinen A, Iwata S, Wikström M (2000) The structure of the ubiquinol oxidase from Escherichia coli and its ubiquinone binding site. Nat Struct Biol 7: 910-917

Pubmed: Author and Title
CrossRef: Author and Title
Google Scholar: Author Only Title Only Author and Title

Allahverdiyeva Y, Ermakova M, Eisenhut M, Zhang P, Richaud P, Hagemann M, Cournac L, Aro EM (2011) Interplay between flavodiiron proteins and photorespiration in Synechocystis sp. PCC 6803. J Biol Chem 286: 24007-24014

Pubmed: Author and Title
CrossRef: Author and Title
Google Scholar: Author Only Title Only Author and Title

Allahverdiyeva Y, Mustila H, Ermakova M, Bersanini L, Richaud P, Ajlani G, Battchikova N, Cournac L, Aro EM (2013) Flavodiiron proteins Flv1 and Flv3 enable cyanobacterial growth and photosynthesis under fluctuating light in aquatic environments. Proc Natl Acad Sci USA 110: 4111-4116

Pubmed: Author and Title
CrossRef: Author and Title
Google Scholar: Author Only Title Only Author and Title

Ardelean II, Peschek GA (2011) The Site of Respiratory Electron Transport in Cyanobacteria and Its Implication for the Photo-Inhibition of Respiration In Peschek GA, Obinger C, Renger G, eds, Bioenergetic processes of cyanobacteria - from evolutionary singularity to ecological diversity, Springer, New York, pp 131-136

Bailey S, Melis A, Mackey KR, Cardol P, Finazzi G, van Dijken G, Berg GM, Arrigo K, Shrager J, Grossman A (2008) Alternative photosynthetic electron flow to oxygen in marine Synechococcus. Biochim Biophys Acta 1777: 269-276

Pubmed: Author and Title
CrossRef: Author and Title
Google Scholar: Author Only Title Only Author and Title

Beckmann K, Messinger J, Badger M, Wydrzynski T, Hillier W (2009) On-line mass spectrometry: membrane inlet sampling. Photosynth Res 102: 511-522

Pubmed: Author and Title
CrossRef: Author and Title
Google Scholar: Author Only Title Only Author and Title

Belatik A, Joly D, Hotchandani S, Carpentier R (2013) Re-evaluation of the side effects of cytochrome b6f inhibitor dibromothymoquinone on photosystem II excitation and electron

transfer. Photosynth Res 117: 489-496

Berry S, Schneider D, Vermaas W, Rogner M (2002) Electron transport routes in whole cells of Synechocystis sp. strain PCC 6803: the role of the cytochrome bd-type oxidase. Biochemistry 41: 3422-3429

Pubmed: Author and Title
CrossRef: Author and Title
Google Scholar: Author Only Title Only Author and Title

Bukhov N, Sridharan G, Egorova E, Carpentier R (2003) Interaction of exogenous quinones with membranes of higher plant chloroplasts: modulation of quinone capacities as photochemical and non-photochemical quenchers of energy in Photosystem II during light-dark transitions. Biochim Biophys Acta 1604: 115-123

Pubmed: Author and Title
CrossRef: Author and Title
Google Scholar: Author Only Title Only Author and Title

Brändén G, Gennisb RB, Brzezinskia P (2006) Transmembrane proton translocation by cytochrome c oxidase. Biochim Biophys Acta 1757: 1052-1063

Pubmed: Author and Title
CrossRef: Author and Title
Google Scholar: Author Only Title Only Author and Title

Cooley JW, Howitt CA, Vermaas W (2000) Succinate:Quinol oxidoreductases in the cyanobacterium Synechocystis sp. srain PCC 6803: presence and function in metabolism and electron transport. J Bacteriol 182: 714-722

Pubmed: Author and Title
CrossRef: Author and Title
Google Scholar: Author Only Title Only Author and Title

Deák Z, Sass L, Kiss E, Vass I (2014) Characterization of wave phenomena in the relaxation of flash-induced chlorophyll fluorescence yield in cyanobacteria. Biochim Biophys Acta 1837: 1522-32

Pubmed: Author and Title
CrossRef: Author and Title
Google Scholar: Author Only Title Only Author and Title

Eisenhut M, Kahlon S, Hasse D, Ewald R, Lieman-Hurwitz J, Ogawa T, Ruth W, Bauwe H, Kaplan A, Hagemann M (2006) The plantlike C2 glycolate cycle and the bacterial-like glycerate pathway cooperate in phosphoglycolate metabolism in cyanobacteria. Plant Physiol 142: 333-342

Pubmed: Author and Title
CrossRef: Author and Title
Google Scholar: Author Only Title Only Author and Title

Eisenhut M, Ruth W, Haimovich M, Bauwe H, Kaplan A, Hagemann M (2008) The photorespiratory glycolate metabolism is essential for cyanobacteria and might have been conveyed endosymbiontically to plants. Proc Natl Acad Sci USA 105: 17199-17204
Pubmed: Author and Title
CrossRef: Author and Title
Google Scholar: Author Only Title Only Author and Title

Ermakova M, Battchikova N, Richaud P, Leino H, Kosourov S, Isojärvi J, Peltier G, Flores E, Cournac L, Allahverdiyeva Y, Aro EM (2014) Heterocystspecific flavodiiron protein Flv3B enables oxic diazotrophic growth of the filamentous cyanobacterium Anabaena sp. PCC 7120. Proc Natl Acad Sci USA 111: 11205-11210
Pubmed: Author and Title
CrossRef: Author and Title
Google Scholar: Author Only Title Only Author and Title

Feilke K, Yu Q, Beyer P,Sétif P, Krieger-Liszkay A (2014) In vitro analysis of the plastid terminal oxidase in photosynthetic electron transport. Biochim Biophys Acta 1837: 1684-1690.
Pubmed: Author and Title
CrossRef: Author and Title
Google Scholar: Author Only Title Only Author and Title

Graan T, Ort DJ (1986) Detection of oxygen-evolving photosystem II centers inactive in plastoquinone reduction. Biochim Biophys Acta 852: 320-330
Pubmed: Author and Title
CrossRef: Author and Title
Google Scholar: Author Only Title Only Author and Title

Hart SE, Schlarb-Ridley BG, Bendall DS, Howe CJ (2005) Terminal oxidases of cyanobacteria. Biochem Soc Trans 33: 832-835
Pubmed: Author and Title
CrossRef: Author and Title
Google Scholar: Author Only Title Only Author and Title

Helman Y, Barkan E, Eisenstadt D, Luz B, Kaplan A (2005) Fractionation of the three stable oxygen isotopes by oxygen-producing and oxygen consuming reactions in photosynthetic organisms. Plant Physiol 138: 2292-2298
Pubmed: Author and Title
CrossRef: Author and Title
Google Scholar: Author Only Title Only Author and Title

Helman Y, Tchernov D, Reinhold L, ShibataM, Ogawa T, Schwarz R, Ohad I, Kaplan A (2003) Genes encoding A-type flavoproteins are essential for photoreduction of O2 in cyanobacteria. Curr Biol 13: 230-235
Pubmed: Author and Title
CrossRef: Author and Title
Google Scholar: Author Only Title Only Author and Title

Heyno E, Gross C, Laureau C, Culcasi M, Pietri S, Krieger-Liszkay A (2009) Plastid Alternative Oxidase (PTOX) Promotes Oxidative Stress When Overexpressed in Tobacco. J. Biol. Chem. 284: 31174-31180.
Pubmed: Author and Title
CrossRef: Author and Title
Google Scholar: Author Only Title Only Author and Title

Hihara Y, Sonoike K, Kanehisa M, Ikeuchi M (2003) DNA microarray analysis of redox-responsive genes in the genome of the cyanobacterium Synechocystis sp. strain PCC 6803. J Bacteriol 185: 1719-1725.
Pubmed: Author and Title
CrossRef: Author and Title
Google Scholar: Author Only Title Only Author and Title

Howitt C, Cooley J, Wiskich J, Vermaas W (2001) A strain of Synechocystis sp. PCC 6803 without photosynthetic oxygen evolution and respiratory oxygen consumption: implications for the study of cyclic photosynthetic electron transport. Planta 214: 46-56.
Pubmed: Author and Title
CrossRef: Author and Title
Google Scholar: Author Only Title Only Author and Title

Howitt C, Udall P, Vermaas W (1999) Type 2 NADH dehydrogenases in the cyanobacterium Synechocystis sp. strain PCC 6803 are involved in regulation rather than respiration. J Bacteriol 181: 3994-4003
Pubmed: Author and Title
CrossRef: Author and Title
Google Scholar: Author Only Title Only Author and Title

Howitt C, Vermaas WF (1998) Quinol and cytochrome oxidases in the cyanobacterium Synechocystis sp. PCC 6803. Biochemistry 37: 17944-17951
Pubmed: Author and Title
CrossRef: Author and Title
Google Scholar: Author Only Title Only Author and Title

Huang C, Yuan X, Zhao J, Bryant DA (2003) Kinetic analyses of state transitions of the cyanobacterium Synechococcus sp. PCC 7002 and its mutant strains impaired in electron transport. Biochim Biophys Acta 1607: 121-130
Pubmed: Author and Title
CrossRef: Author and Title
Google Scholar: Author Only Title Only Author and Title

Huang F, Parmryd I, Nilsson F, Persson AL, Pakrasi HB, Andersson B, Norling B (2002) Proteomics of Synechocystis sp. strain PCC 6803: identification of plasma membrane proteins. Mol Cell Proteomics 1: 956-966.

Pubmed: Author and Title
CrossRef: Author and Title
Google Scholar: Author Only Title Only Author and Title

Iwata S, Ostermeier C, Ludwig B, Michel H (1995) Structure at 2.8-Angstrom Resolution of Cytochrome-C-Oxidase from Paracoccus-Denitrificans. Nature 376: 660-669
Pubmed: Author and Title
CrossRef: Author and Title
Google Scholar: Author Only Title Only Author and Title

Joliot P, Johnson GN (2011) Regulation of cyclic and linear electron flow in higher plants. Proc Natl Acad Sci 108: 13317-13322
Pubmed: Author and Title
CrossRef: Author and Title
Google Scholar: Author Only Title Only Author and Title

Kok B (1949) On the interrelation of respiration and photosynthesis in green plants. Biochim Biophys Acta 3: 625-631
Pubmed: Author and Title
CrossRef: Author and Title
Google Scholar: Author Only Title Only Author and Title

Kranzler C, Lis H, Finkel OM, Schmetterer G, Shaked Y, Keren N (2014) Coordinated transporter activity shapes high-affinity iron acquisition in cyanobacteria. ISME J 8: 409-417
Pubmed: Author and Title
CrossRef: Author and Title
Google Scholar: Author Only Title Only Author and Title

Kufryk G, Vermaas W (2006) Sll1717 in Synechocystis sp. PCC 6803 affects the redox state of the plastoquinone pool by modulating quinol oxidase activity in thylakoids. J. Bacteriol 188: 1286-1294
Pubmed: Author and Title
CrossRef: Author and Title
Google Scholar: Author Only Title Only Author and Title

Lea-Smith DJ, Bombelli P, Vasudevan R, Howe C (2016) Photosynthetic, respiratory and extracellular electron transport pathways in cyanobacteria. Biochim Biophys Acta 1857: 247-255
Pubmed: Author and Title
CrossRef: Author and Title
Google Scholar: Author Only Title Only Author and Title

Lea-Smith DJ, Ross N, Zori M, Bendall DS, Dennis JS, Scott SA, Smith AG, Howe CJ (2013) Thylakoid terminal oxidases are essential for the cyanobacterium Synechocystis sp. PCC 6803 to survive rapidly changing light intensities. Plant Physiol 162: 484-495
Pubmed: Author and Title
CrossRef: Author and Title
Google Scholar: Author Only Title Only Author and Title

Liu LN, Bryan SJ, Huang F, Yu J, Nixon PJ, Rich PR, Mullineaux CW (2012) Control of electron transport routes through redox-regulated redistribution of respiratory complexes. Proc Natl Acad Sci USA 109: 11431-11436
Pubmed: Author and Title
CrossRef: Author and Title
Google Scholar: Author Only Title Only Author and Title

Matthijs HC, Lubberding HJ (1988) Dark respiration in cyanobacteria. In LJ Rogers, JR Gallon, eds, Biochemistry of the Algae and Cyanobacteria. Clarendon Press, Oxford, pp 131-145
Pubmed: Author and Title
CrossRef: Author and Title
Google Scholar: Author Only Title Only Author and Title

McDonald AE, Ivanov AG, Bode R, Maxwell DP, Rodermel SR, Huner NP (2011) Flexibility in photosynthetic electron transport: the physiological role of plastoquinol terminal oxidase (PTOX). Biochim Biophys Acta 1807: 954-967
Pubmed: Author and Title
CrossRef: Author and Title
Google Scholar: Author Only Title Only Author and Title

Mi H, Endo T, Schreiber U, Ogawa T, Asada K (1992) Electron donation from cyclic and respiratory flows to the photosynthetic intersystem chain is mediated by pyridine nucleotide dehydrogenase in the cyanobacterium Synechocystis PCC 6803. Plant Cell Physiol 33: 1233-1237
Pubmed: Author and Title
CrossRef: Author and Title
Google Scholar: Author Only Title Only Author and Title

Mullineaux CW (2014a) Co-existence of photosynthetic and respiratory activities in cyanobacterial thylakoid membranes. Biochim Biophys Acta 1837: 503-511
Pubmed: Author and Title
CrossRef: Author and Title
Google Scholar: Author Only Title Only Author and Title

Mullineaux CW (2014b) Electron transport and light-harvesting switches in cyanobacteria. Front Plant Sci 5: 7
Pubmed: Author and Title
CrossRef: Author and Title
Google Scholar: Author Only Title Only Author and Title

Mullineaux CW, Allen JF (1986) The state 2 transition in the cyanobacterium Synechococcus 6301 can be driven by respiratory electron flow into the plastoquinone pool. FEBS Lett 205: 155-160
Pubmed: Author and Title
CrossRef: Author and Title
Google Scholar: Author Only Title Only Author and Title

Mustila H, Paananen P, Battchikova N, Santana-Sanchez A, Muth-Pawlak D, Hagemann M, Aro EM, Allahverdiyeva Y (2016) The Flavodiiron Protein Flv3 functions as a homo-oligomer during stress acclimation and is distinct from the Flv1/Flv3 hetero-oligomer specific to the O2 photoreduction pathway. Plant and Cell Phys doi: 10.1093/pcp/pcw047
Pubmed: Author and Title
CrossRef: Author and Title
Google Scholar: Author Only Title Only Author and Title

Nishio JN, Whitmarsh J (1993) Dissipation of the proton gradient in intact chlorophasts. II. The pH gradient monitored by cytochrome f reduction kinetics. Plant Physiol 101: 89-96
Pubmed: Author and Title
CrossRef: Author and Title
Google Scholar: Author Only Title Only Author and Title

Nomura CT, Persson S, Shen G, Inoue-Sakamoto K, Bryant DA (2006) Characterization of two cytochrome oxidase operons in the marine cyanobacterium Synechococcus sp. PCC 7002: inactivation of ctaDI affects the PSI:PSII ratio. Photosyn Res 87: 215-228
Pubmed: Author and Title
CrossRef: Author and Title
Google Scholar: Author Only Title Only Author and Title

Ohkawa H, Pakrasi HB, Ogawa T (2000) Two types of functionally distinct NAD(P)Hdehydrogenases in Synechocystis sp. strain PCC6803. J. Biol. Chem 275: 31630-31634
Pubmed: Author and Title
CrossRef: Author and Title
Google Scholar: Author Only Title Only Author and Title

Pils D, Gregor W, Schmetterer G (1997) Evidence for in vivo activity of three distinct respiratory terminal oxidases in the cyanobacterium Synechocystis sp. strain PCC6803. FEMS Microbiol 152: 83-88
Pubmed: Author and Title
CrossRef: Author and Title
Google Scholar: Author Only Title Only Author and Title

Pils D, Schmetterer G (2001) Characterization of three bioenergetically active respiratory terminal oxidases in the cyanobacterium Synechocystis sp. strain PCC 6803. FEMS Microbiol Lett 203: 217-22
Pubmed: Author and Title
CrossRef: Author and Title
Google Scholar: Author Only Title Only Author and Title

Pisareva T, Shumskaya M, Maddalo G, Ilag L, Norling B (2007) Proteomics of Synechocystis sp PCC 6803 - Identification of novel integral plasma membrane proteins. FEBS J 274: 791-804.
Pubmed: Author and Title
CrossRef: Author and Title
Google Scholar: Author Only Title Only Author and Title

Scherer S (1990) Do photosynthetic and respiratory electron transport chains share redox proteins? Trends Biochem Sci 15: 458-62
Pubmed: Author and Title
CrossRef: Author and Title
Google Scholar: Author Only Title Only Author and Title

Schneider D, Berry S, Rich P, Seidler A, Rögner M (2001) A regulatory role of the PetM subunit in a cyanobacterial cytochrome b6f complex. J Biol Chem 276:16780-16785
Pubmed: Author and Title
CrossRef: Author and Title
Google Scholar: Author Only Title Only Author and Title

Schneider D, Berry S, Volkmer T, Seidler A, Rögner M (2004) PetC1 is the major Rieske iron-sulfur protein in the cytochrome b6f complex of Synechocystis sp. PCC 6803. J Biol Chem 279: 39383-39388
Pubmed: Author and Title
CrossRef: Author and Title
Google Scholar: Author Only Title Only Author and Title

Schultze M, Forberich B, Rexroth S, Dyczmons N, Roegner M, Appel J (2009) Localization of cytochrome b(6)f complexes implies an incomplete respiratory chain in cytoplasmic membranes of the cyanobacterium Synechocystis sp. PCC 6803. Biochim Biophys Acta 1787: 1479-1485
Pubmed: Author and Title
CrossRef: Author and Title
Google Scholar: Author Only Title Only Author and Title

Schuurmans RM, Schuurmans JM, Bekker M, Kromkamp JC, Matthijs HCP, Hellingwerf KJ (2014) The redox potential of the plastoquinone pool of the cyanobacterium Synechocystis species strain PCC 6803 is under strict homeostatic control. Plant Physiol 165: 463-475
Pubmed: Author and Title
CrossRef: Author and Title
Google Scholar: Author Only Title Only Author and Title

Shen G, Boussiba S, Vermaas WFJ (1993) Synechocystis sp. PCC 6803 strains lacking photosystem I and phycobilisome function. Plant Cell 5: 1853-1863
Pubmed: Author and Title
CrossRef: Author and Title
Google Scholar: Author Only Title Only Author and Title

Suorsa M, Grieco M, Järvi S, Gollan PJ, Kangasjärvi S, Tikkanen M, Aro EM (2013) PGR5 ensures photosynthetic control to safeguard photosystem I under fluctuating light conditions. Plant Signal Behav 8: e22741
Pubmed: Author and Title
CrossRef: Author and Title
Google Scholar: Author Only Title Only Author and Title

Trebst A, Harth E, Draber W (1970) on a new inhibitor of photosynthetic electron-transport in isolated chloroplasts. Z Naturforsch 25: 1157-1159
Pubmed: Author and Title
CrossRef: Author and Title
Google Scholar: Author Only Title Only Author and Title

Tsunoyama Y, Bernát G, Dyczmons NG, Schneider D, Rögner M (2009) Multiple Rieske proteins enable short- and long-term light adaptation of Synechocystis sp. PCC 6803. J Biol Chem 284: 27875-27883
Pubmed: Author and Title
CrossRef: Author and Title
Google Scholar: Author Only Title Only Author and Title

Vass I, Kirilovsky D and Etienne A-L (1999) UV-B radiation- induced donor and acceptor side modifications of Photosystem II in the cyanobacterium Synechocystis sp.PCC 6803. Biochemistry 38: 12786-12794
Pubmed: Author and Title
CrossRef: Author and Title
Google Scholar: Author Only Title Only Author and Title

Vermaas W (2001) Photosynthesis and Respiration in Cyanobacteria. eLS.
Pubmed: Author and Title
CrossRef: Author and Title
Google Scholar: Author Only Title Only Author and Title

Vicente JB, Gomes CM, Wasserfallen A, Teixeira M (2002) Module fusion in an A-type flavoprotein from the cyanobacterium Synechocystis condenses a multiple-component pathway in a single polypeptide chain. Biochem Biophys Res Commun 294: 82-87
Pubmed: Author and Title
CrossRef: Author and Title
Google Scholar: Author Only Title Only Author and Title

Yan J, Kurisu G, Cramer WA (2006) Intraprotein transfer of the quinone analogue inhibitor 2,5-dibromo-3-methyl-6-isopropyl-pbenzoquinone in the cytochrome b6f complex. Proc Natl Acad Sci USA 103: 169-174
Pubmed: Author and Title
CrossRef: Author and Title
Google Scholar: Author Only Title Only Author and Title

Yu Q, Feilke K, Krieger-Liszkay A, Beyer P (2014) Functional and molecular characterization of plastid terminal oxidase from rice (Oryza sativa) Biochim Biophys Acta 1837: 1284-1292.
Pubmed: Author and Title
CrossRef: Author and Title
Google Scholar: Author Only Title Only Author and Title

Zhang L, Selão TT, Pisareva T, Qian J, Sze SK, Carlberg I, Norling B (2013) Deletion of Synechocystis sp. PCC 6803 leader peptidase LepB1 affects photosynthetic complexes and respiration. Mol Cell Proteomics 12: 1192-1203
Pubmed: Author and Title
CrossRef: Author and Title
Google Scholar: Author Only Title Only Author and Title

Zhang P, Allahverdiyeva Y, Eisenhut M, Aro EM (2009) Flavodiiron proteins in oxygenic photosynthetic organisms: Photoprotection of photosystem II by Flv2 and Flv4 in Synechocystis sp. PCC 6803. PLoS ONE 4: e5331
Pubmed: Author and Title
CrossRef: Author and Title
Google Scholar: Author Only Title Only Author and Title

MATERIALS AND METHODS

Oxygen Evolution Measurements with a Clark-type oxygen electrode

The effect of different DBMIB concentrations on the net O_2 production was measured with a Clark-type oxygen electrode (Hansatech Ltd, Norfolk, England) at 30°C under 400 μmol photons m^{-2} s^{-1} actinic light applied via a 150 Watt, 21 V, EKE quartz halogen-powered fiber optic illuminator (Fiber-Lite DC-950, Dolan-Jenner, MA, USA). Before measurements the cells were collected and resuspended in fresh growth medium at a chlorophyll concentration of 15 μg mL^{-1}. All the measurements were performed in the presence of 1 mM $NaHCO_3$.

MATERIALS AND METHODS

Oxygen Evolution Measurements with a Clark-type oxygen electrode

The effect of different DBMIB concentrations on the net O_2 production was measured with a Clark-type oxygen electrode (Hansatech Ltd, Norfolk, England) at 30°C under 400 μmol photons m^{-2} s^{-1} actinic light applied via a 150 Watt, 21 V, EKE quartz halogen-powered fiber optic illuminator (Fiber-Lite DC-950, Dolan-Jenner, MA, USA). Before measurements the cells were collected and resuspended in fresh growth medium at a chlorophyll concentration of 15 μg mL^{-1}. All the measurements were performed in the presence of 1 mM $NaHCO_3$.

FIGURES

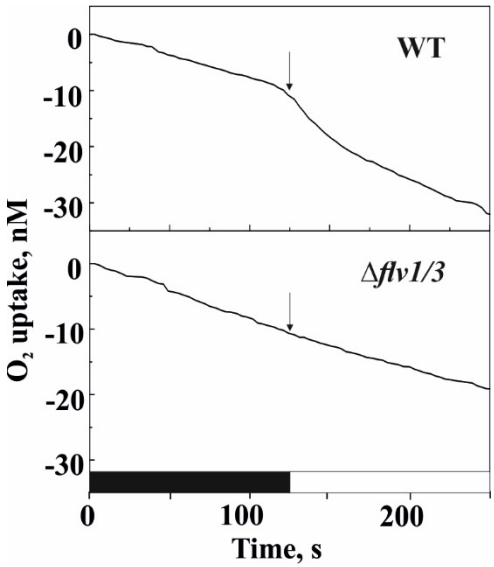

Figure S1. MIMS analysis of O_2 uptake by WT and Δ*flv1/3* cells during dark to light transition. Arrows indicate the beginning of illumination with a strong white light at an intensity of 400 μmol photons m^{-2} s^{-1}. The slope of the curves does not provide a precise quantitative measure of the rate of O_2 consumption until it is corrected for the isotopic ratio ($^{16}O/^{18}O$).

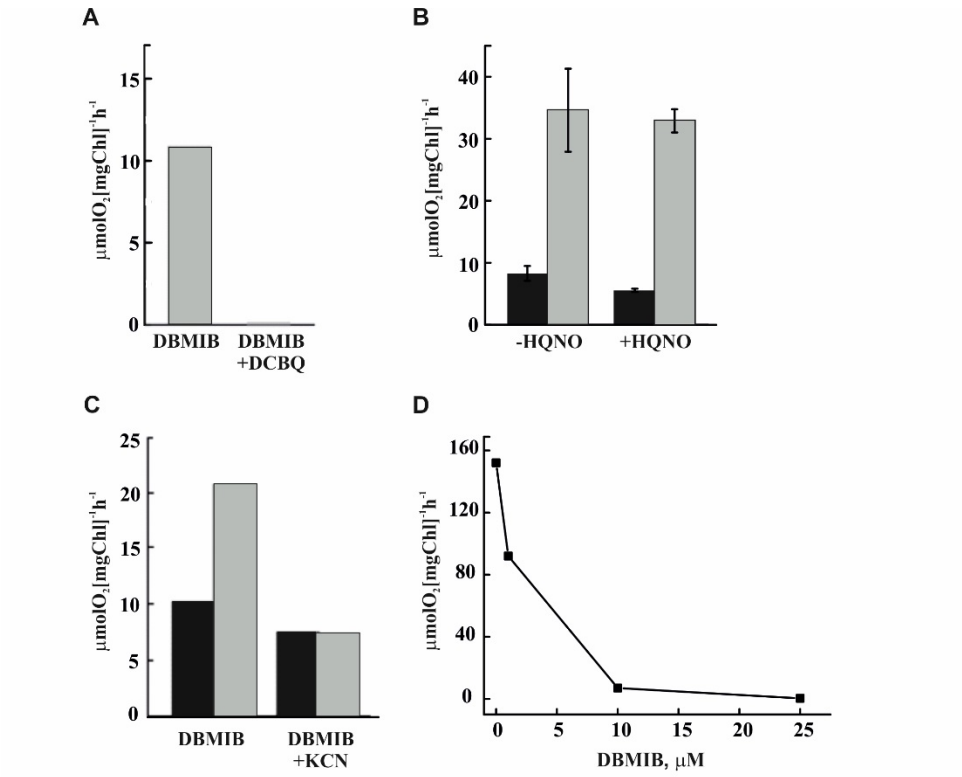

Figure S2. The rates of O_2 uptake and O_2 production in WT *Synechocystis* cells: (A) Light-induced O_2 uptake in the presence of DBMIB and DBMIB+DCBQ; (B) Total O_2 uptake in darkness (black bars) and in the light (grey bars) without and in the presence of HQNO, mean ± SD, n=3-4; (C) Total O_2 uptake in darkness (black bars) and in the light (grey bars) in the presence of DBMIB or DBMIB+KCN and (D) Net O_2 production in the presence of increasing DBMIB concentrations.

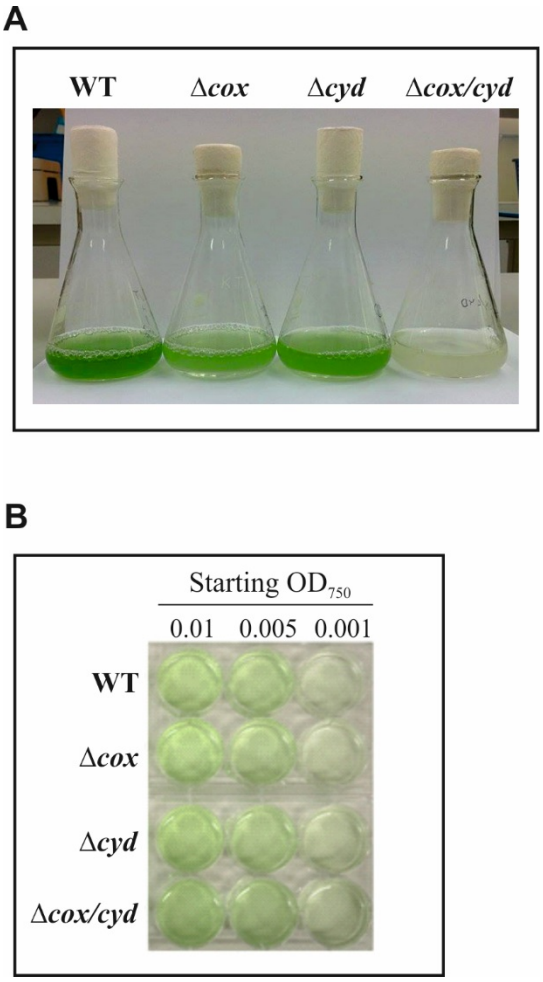

Figure S3. The growth of *Synechocystis* WT and RTO-deficient mutant cells under different light conditions: (A) 12 h dark / 12 h high light (200 μmol photons m^{-2} s^{-1}) square cycles for 8 days; (B) constant high light at an intensity of 500 μmol photons m^{-2} s^{-1} for 2 days.

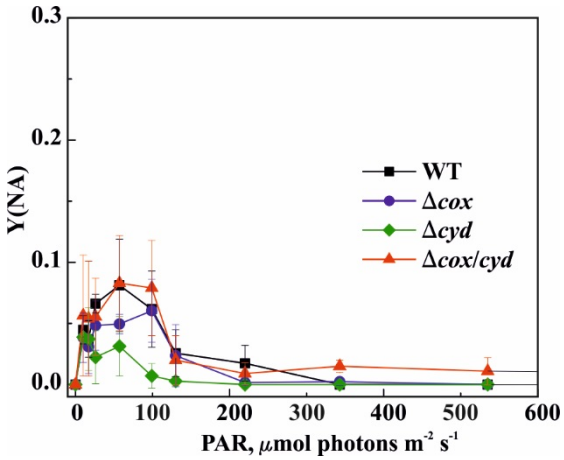

Figure S4. Acceptor side limitation of PS I Y(NA) of the WT and RTO-deficient mutants calculated from the rapid light curves. Mean ± SD, n=3.

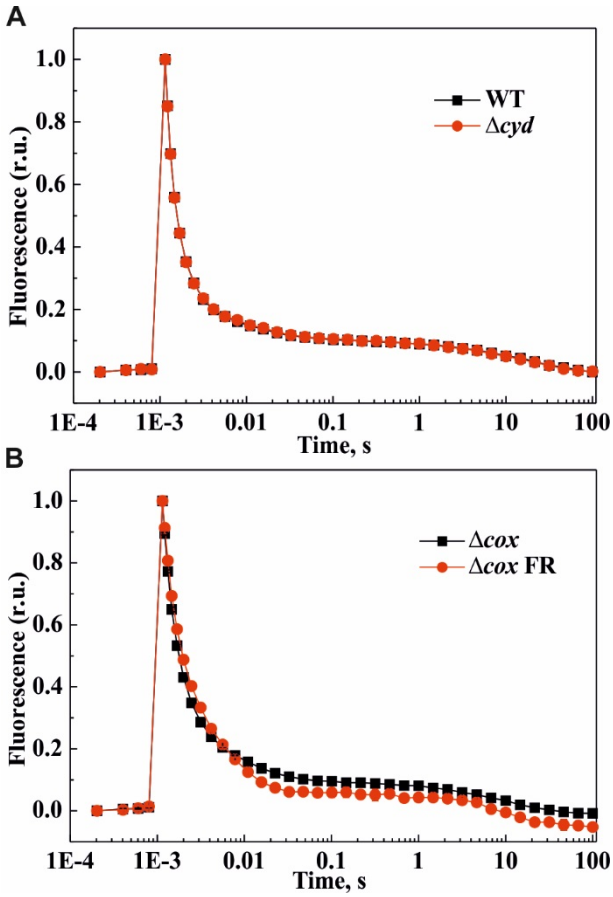

Figure S5. Relaxation of the flash-induced fluorescence yield from WT and RTO mutants: (A) WT and Δ*cyd* cells were dark-adapted for 5 min before the experiment; (B) Δ*cox* cells were dark-adapted for 5 min or pre-illuminated by far-red light before the experiment. Mean ± SD, n=2-3. Curves were normalized to the same amplitude to facilitate comparison of the kinetics.

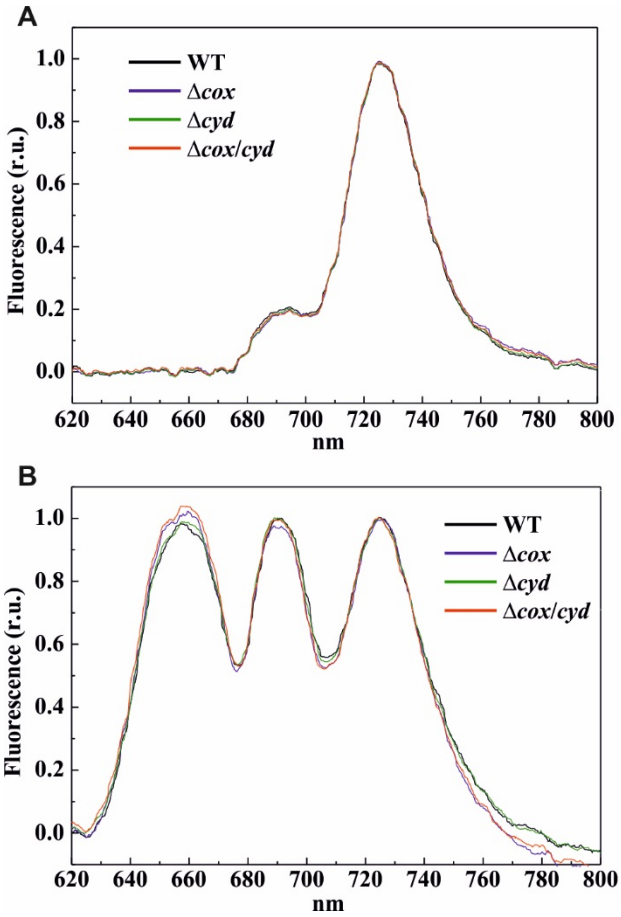

Figure S6. Fluorescence emission spectra recorded at 77K : (A) from the cells excited with 580-nm light; (B) from the cells excited with 440-nm light.

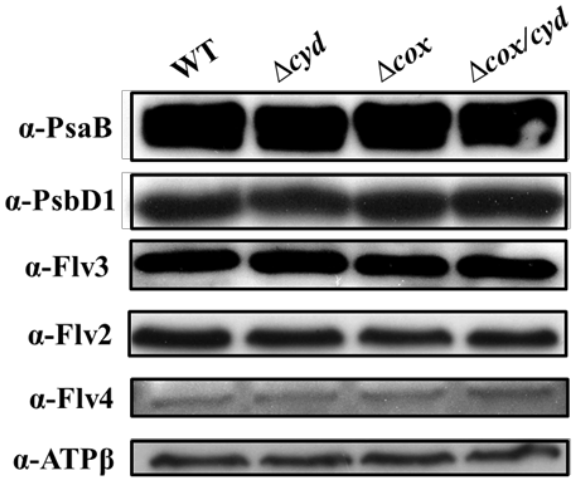

Figure S7. Protein analysis of the WT *Synechocystis* and RTO-deficient mutants.

MATERIALS AND METHODS

Oxygen Evolution Measurements with a Clark-type oxygen electrode

The effect of different DBMIB concentrations on the net O_2 production was measured with a Clark-type oxygen electrode (Hansatech Ltd, Norfolk, England) at 30°C under 400 μmol photons m^{-2} s^{-1} actinic light applied via a 150 Watt, 21 V, EKE quartz halogen-powered fiber optic illuminator (Fiber-Lite DC-950, Dolan-Jenner, MA, USA). Before measurements the cells were collected and resuspended in fresh growth medium at a chlorophyll concentration of 15 μg mL^{-1}. All the measurements were performed in the presence of 1 mM $NaHCO_3$.